

LÉVY SCORE FUNCTION AND SCORE-BASED PARTICLE ALGORITHM FOR NONLINEAR LÉVY–FOKKER–PLANCK EQUATIONS*

YUANFEI HUANG[†], CHENGYU LIU[‡], AND XIANG ZHOU[§]

Abstract. The score function for the diffusion process, also known as the gradient of the log-density, is a basic concept to characterize the probability flow with important applications in the score-based diffusion generative modelling and the simulation of Itô stochastic differential equations. However, neither the probability flow nor the corresponding score function for the diffusion-jump process are known. This paper delivers mathematical derivation, numerical algorithm, and error analysis focusing on the corresponding score function in non-Gaussian systems with jumps and discontinuities represented by the nonlinear Lévy–Fokker–Planck equations. We propose the Lévy score function for such stochastic equations, which features a nonlocal double-integral term, and we develop its training algorithm by minimizing the proposed loss function from samples. Based on the equivalence of the probability flow with deterministic dynamics, we develop a self-consistent score-based transport particle algorithm to sample the interactive Lévy stochastic process at discrete time grid points. We provide error bound for the Kullback–Leibler divergence between the numerical and true probability density functions by overcoming the nonlocal challenges in the Lévy score. The full error analysis with the Monte Carlo error and the time discretization error is furthermore established. To show the usefulness and efficiency of our approach, numerical examples from applications in biology and finance are tested.

Key words. score function; stochastic differential equation; Lévy–Fokker–Planck equation; probability flow; score-based particle method; Lévy noise.

MSC codes. 65M75, 65C35, 68T07, 60H35

1. Introduction. Stochastic processes, such as the Itô diffusion process and the Lévy jump process, play prominent roles in a variety range of fields including science, engineering, economics, and statistics. The temporal evolution of the probability distribution, satisfying the initial-value forward Kolmogorov equation, can be also viewed as a path or curve in the space of probability distributions. The path connecting two probability density functions associated certain stochastic processes is the crucial mathematical tool the basis of score-based generative algorithms [38].

The viewpoint of probability flow is to treat the time evolution of the probability density function as the continuity equation whose velocity field contains the gradient of the density function in the self-consistent way. In the setting of a diffusion process X_t , the density function p_t of X_t is given by the Fokker-Planck equation

$$(1.1) \quad \frac{\partial p_t(x)}{\partial t} = -\nabla \cdot \left[\underbrace{\left(b(x, t) - \frac{1}{2} \nabla \cdot \Sigma(x, t) - \frac{1}{2} \Sigma(x, t) \nabla \log p_t(x) \right)}_{v(x, t)} p_t(x) \right],$$

where b is the drift term and Σ corresponds to the diffusion matrix. If the term

*Submitted to the editors DATE.

Funding: This work was funded by the Hong Kong General Research Funds (11308121, 11318522, 11308323), and the NSFC/RGC Joint Research Scheme [RGC Project No. N-CityU102/20 and NSFC Project No. 12061160462].

[†]Department of Data Science, City University of Hong Kong, Kowloon, Hong Kong SAR, (yhuan26@cityu.edu.hk).

[‡]Department of Data Science, City University of Hong Kong, Kowloon, Hong Kong SAR, (cliu687-c@my.cityu.edu.hk).

[§]Department of Mathematics, City University of Hong Kong, Kowloon, Hong Kong SAR, (xizhou@cityu.edu.hk)

$\nabla \log p_t$, denoted by the score function $s_t(x)$, is *known a priori*, then (1.1) takes the form of a continuity equation corresponds to the transportation between the density functions p_0 and p_T by a underlying deterministic ODE flow with the new vector field $v(x, t) := b(x, t) - 1/2\nabla \cdot \Sigma(x, t) - 1/2\Sigma(x, t)s_t(x)$. This observation is also the theoretic foundation of reversing a Markov diffusion process in score-based diffusion models since the time reverse from p_T to p_0 can implemented by the time-reversed deterministic flow. However, the various numerical methods [19, 36, 38, 34] to find the score function s_t for the generative modeling like image synthesis are limited to the constant drift or the Orenstein-Uhlenbeck process, because these simple processes suffice to inject Gaussian noise to the data. In such simple systems, the transition probability is analytically available.

Motivated by the probability flow and score-based generative models, a number of studies [29, 33, 24, 28, 4, 32] have been recently carried out to learn the *underlying velocity field* $v(x, t)$ that drives the probability density function in Fokker-Planck equations, instead of directly simulating the diffusion SDE or solving the Fokker-Planck PDE. These methods, usually referred to as *score-based transport modeling*[4], deterministically push samples from the initial density onto samples from the solution at any later time by employing particle methods to learn the score function from the samples following the deterministic flow. By finding the above mentioned score function appearing in the new velocity field, this numerical strategy works well due to the self-consistency of the Fokker-Planck equation [24, 24] in the form of fixed-point argument. Compared with the traditional grid-based numerical methods for the Fokker-Planck equation, these score-based methods can scale well in high dimensions. Compared to the traditional numerical SDE schemes, the deterministic flow is faster to compute and offers the expression of the density function to facilitate calculating many non-equilibrium statistical quantities like the probability current, the entropy production rate and the heat [39, 5]. The theoretic works related to these algorithms include the error analysis for Kullback-Leibler divergence due to the approximate score function [32, 33, 28, 4]. There are also substantial extensions from the Fokker-Planck equation to the McKean-Vlaso equation [29, 32, 28] and the Fokker-Planck-Landau equation[20, 17].

However, the existing score-based transport modeling only studied the diffusion process with the focus on the conventional score function $s_t = \nabla \log p_t$ and the score matching error $\int_{t_0}^T \int_{\Omega} |s^\theta(x, t) - \nabla \log p_t(x)|^2 p_t(x) dx dt$ as the loss function to train the score. Despite the popularity in applications of the diffusion model, the non-Gaussian processes such as Lévy processes are preferred to more accurately represent complex stochastic events than conventional Gaussian models [22, 3, 35]. Recently, the Lévy-Itô model with the *fractional* score function $s_t^{(\alpha)}(x) = (\Delta^{\frac{\alpha-2}{2}} \nabla p_t(x))/p_t(x)$, $\alpha \in (1, 2]$, is used in [41] for score-based generative models to generate more diverse samples by taking advantage of the heavy-tailed properties of the α -stable Lévy process. In [16], the same fractional score function is computed for the Lévy-Fokker-Planck equation by training the fractional score-based physics-informed neural networks from a large number of sample stochastic trajectories as the training data.

In this paper, we systematically investigate the score-based transport modeling for the general Markov process of non-Gaussian type and develop the score-based theories and algorithms to simulate the underlying jump-diffusion process. This paper delivers mathematical derivation, numerical algorithm, and error analysis focusing on the corresponding score function in non-Gaussian systems with jumps and discontinuities represented by the nonlinear Lévy-Fokker-Planck equations. We propose the

Lévy score function for such stochastic equations, which features a nonlocal double-integral term, and its training algorithm by minimizing the proposed loss function from samples. Based on the equivalence of the probability flow with deterministic dynamics, we develop a self-consistent score-based transport particle algorithm to sample the interactive Lévy stochastic process at discrete time grid points.

Contributions

1. For the nonlinear stochastic differential equation (2.1) driven by the Brownian and Lévy noise as well as the mean-field interaction, we derive the continuity equation for the nonlinear Lévy-Fokker-Planck equation (2.3) to identify the vector field in the probability flow. We propose the *generalized score function*, \widehat{S}_t in (2.7), consisting of both the conventional diffusion score function $\nabla \log p_t$ and the *Lévy score function*. The latter has the non-local double-integral terms involving the Lévy measure.
2. We show in Theorem 3.2 that, the Kullback–Leibler divergence $\sup_{t \in [t_0, T]} D_{\text{KL}}(p_t^\theta \| \widehat{p}_t)$ between the numerical score-based p_t^θ and the true density function \widehat{p}_t is bounded by a loss function we derived from the fixed-point argument. This is a significant extension to [32, 33, 4, 28] since our analysis takes into account of both the non-Gaussian process and the mean-field interactions.
3. We propose the score-matching training algorithm to learn both the diffusion and Lévy score functions by one single neural network, then develop the sequential score-based particle algorithm (**Algorithm 3.1**) to solve the Lévy-Fokker-Planck equation based on the idea of score-based transport modeling. We test several numerical examples to demonstrate the effectiveness of our approach.
4. We prove in Theorem 3.4 the numerical error of **Algorithm 3.1** for solving (2.1): $\frac{1}{T} \mathbb{E} |X_{n\Delta t}^* - X_{n\Delta t}^N| \leq \mathcal{O}\left(\frac{1}{\sqrt{N}}\right) + \mathcal{O}(\varepsilon) + \mathcal{O}(\Delta t)$, with N the number of particles, ε the bounds of score loss, and Δt the time step size, $n\Delta t \leq T$.

Related works:

Score-based diffusion model and the error analysis. The score-based diffusion model is formulated as the forward and backward continuous Itô stochastic differential equations in [38]. The score matching to train the score function by neural networks includes [19, 37, 15, 34, 14, 27]. For comprehensive reviews on related topics, we refer readers to [12]. There are also extensive works to analyze the convergence and error estimates, for instance [10, 8, 7].

Score-based transport modeling for Fokker-Planck equation. These methods are all based on (1.1) – the equivalence to probability flow – to simulate the time evolution of Fokker-Planck solutions. [29] runs a large number of interacting deterministic particles where the gradient-log-density (score) function is approximated in the reproducing kernel Hilbert space (RKHS). [33, 32] formulated a fixed-point problem for the self-consistency of the probability flow for the Fokker-Planck equation, but the optimization for the diffusion score function is based on the adjoint method which is in general slow and challenging to implement. The score-based transport modeling in [4] is to march the flow sequentially in time with the forward Euler scheme. Instead, [24] proposed to learn the velocity field $v(t, x)$ as a whole for $t \in [0, T]$ by an iterative update of the velocity field.

Score-based generative models with α -stable Lévy processes. [41] proposed score-based generative models with a simple forward Lévy process $X_t = a(t)X_0 + \gamma(t)\epsilon$, where X_0 follows the data distribution, and the noise ϵ follows the isotropic α -stable distribution with the scalar parameter 1. The fractional score function

$s_t^{(\alpha)}(x) = (\Delta^{\frac{\alpha-2}{2}} \nabla p_t(x)) / p_t(x)$ with $1 < \alpha \leq 2$, is proposed for the pdf $p_t(x)$ in order to define the time-reversal Lévy process. This fractional score function is approximated by a neural network and simple enough to use the denoising score-matching similarly to the score-based diffusion models.

Fractional score-based physics-informed neural networks(PINN) for α -stable Lévy processes . [16] proposed the score-fPINN method for the log-likelihood $q_t := \log p_t$ of an α -stable Lévy process by minimizing the PINN loss for the two nonlinear PDEs of q_t and $s_t = \nabla q_t$ respectively, which involve the pairs q and $s^{(\alpha)}$, $s^{(\alpha)}$ and s , respectively, where $s^{(\alpha)}$ is the same fractional score defined as in [41]. The fractional score $s^{(\alpha)}$ serves only as an intermediate variable to compute from s_t to q_t . By the score-matching method applicable to *any* stochastic process [37], the diffusion score $s_t \approx \nabla \log p_t$ is computed by the neural network, entirely based on the *simulated long trajectories* of the SDE beforehand.

Finally, we provide some remarks in the following to further explain a few other aspects of our works.

- We consider a broader range of Lévy processes than the α -stable Lévy process studied in literatures such as [41] and [16]. Our model (2.1) here is far beyond this simple Lévy process, and the corresponding score function is much more intricate than the fractional score function. Refer to Section 2.3.
- Our algorithm and analysis cover the systems with mean-field interactions as in [28, 32]. Our theorems apply to the interaction kernels of the bounded interaction and the Biot-Savart interaction as in [32] for the Fokker–Planck equation. But due to the challenges from the Lévy score, we have not yet prove for the Column interaction as the diffusion process in [32].
- The generalized score function trained in **Algorithm 3.1** contains the contributions of drift, interaction, diffusion and jump; thus, the transport for the N deterministic particles are independent of each other, while [28] still evolves the N interactive particles with the mean-field interaction.
- Even though our numerical algorithm to train the score is sequential in time as in [4], the approach in [24] of the self-consistent velocity matching by learning from the whole simulated trajectories until a terminal time is applicable to the Lévy–Fokker–Planck equation here, because the same fixed-point formulation works with the new defined Lévy score function in our work.

The structure of this paper is as follows: Section 2 shows how to define the generalized score function (the diffusion score and the Lévy score) and establish the probability flow equivalence. Section 3 introduces a particle system-based numerical method, presents bounds on the Kullback–Leibler divergence in Theorem 3.2, and analyzes discretization errors in Theorem 3.4. Section 4 demonstrates the method through numerical experiments. The conclusion part is summarized in Section 5.

2. Probability Flow of Jump-Diffusion and Lévy Score Function.

2.1. McKean–Vlasov SDE driven by Lévy noise. We consider the following McKean–Vlasov stochastic differential equation that incorporates non-Gaussian noise:

$$(2.1) \quad \begin{cases} dX_t = b(X_{t-}, t) dt + (K * \hat{p}_t)(X_{t-}) dt + \sigma(X_{t-}, t) dB_t + \int_{|r| < 1} F(r, t) \tilde{\mathcal{N}}(dt, dr) \\ \quad + \int_{|r| \geq 1} G(r, t) \mathcal{N}(dt, dr), \quad \hat{p}_t = \text{Law}(X_t), \quad X_t \in \Omega, \quad t > t_0, \\ X_{t_0} \sim \mu_0 \in \mathcal{P}_2(\Omega), \end{cases}$$

where $\mathcal{P}_2(\Omega)$ denotes the set of probability measures in Ω with finite quadratic moment and \widehat{p}_t denotes the law of X_t . The domain Ω is either \mathbb{R}^d or the torus \mathbb{T}^d (a hypercube $[-L, L]^d$ with periodic boundary condition), B is a standard Brownian motion in \mathbb{R}^m and \mathcal{N} is an independent Poisson random measure on $\mathbb{R}_+ \times (\mathbb{R}^d \setminus \{0\})$ with the associated compensator $\widetilde{\mathcal{N}}$ and the intensity measure ν which is a Lévy measure, i.e., $\widetilde{\mathcal{N}}(dt, dr) = \mathcal{N}(dt, dr) - \nu(dr) dt$. The mappings $b_i : \mathbb{R}^d \times [t_0, \infty) \rightarrow \mathbb{R}$, $\sigma_{ij} : \mathbb{R}^d \times [t_0, \infty) \rightarrow \mathbb{R}$, $\sigma = (\sigma_{ij})_{d \times m}$, $\Sigma = \sigma \sigma^\top$, $F_i : \mathbb{R}^d \times [t_0, \infty) \rightarrow \mathbb{R}$, $G_i : \mathbb{R}^d \times [t_0, \infty) \rightarrow \mathbb{R}$, all assumed to be measurable for $1 \leq i \leq d$ and $1 \leq j \leq m$. $K : \mathbb{R}^d \rightarrow \mathbb{R}^d$ denotes some interaction kernel and $*$ denotes the convolution operation, i.e., $(K * \widehat{p}_t)(X_t) = \int_{\Omega} K(X_t - y) \widehat{p}_t(y) dy$. We introduce the following assumptions on the drift term b , diffusion coefficient σ , the jump noise coefficients F, G and the Lévy measure ν .

ASSUMPTION 1.

1. For every $t \geq t_0$, $b_i(\cdot, t)$ and $\sigma_{ij}(\cdot, t)$ are C^2 -measurable functions for $1 \leq i \leq d$ and $1 \leq j \leq m$. There exists positive constants C_b, C_σ such that $|b(t, x) - b(t, y)|^2 \leq C_b |x - y|^2$, $(C_\sigma)^{-1} \leq \Sigma_{ij}(x, t) \leq C_\sigma$, $\forall x, y \in \Omega$, $t \geq t_0$, $i, j = 1, \dots, d$, where $|\cdot|$ denotes the Euclidean norm in \mathbb{R}^d .
2. The functions $F, G \in C(\mathbb{R}^d \times [t_0, \infty), \mathbb{R}^d)$, the Lévy measure ν satisfies $\int_{\mathbb{R}^d \setminus \{0\}} (1 \wedge |r|^2) \nu(dr) < \infty$, and there exist constants C_T^F and C_T^G dependent on T such that $\int_{|r| < 1} |F(r, t)|^2 \nu(dr) < C_T^F$, $\int_{|r| \geq 1} |G(r, t)|^2 \nu(dr) < C_T^G$, $\forall t \in [t_0, T]$.

Our analysis will focus on the following two cases of the interaction kernel K .

1. **(Bounded interaction)** The kernel $K \in C^2(\mathbb{R}^d)$ and there exists a positive constant C_K such that $|K(x)| \leq C_K$, $\forall x \in \Omega$.
2. **(Biot–Savart interaction)** The dimension $d = 2$ and the interaction term K is the Biot–Savart kernel, i.e., $K(x) = \frac{1}{2\pi} \left(-\frac{x_2}{|x|^2}, \frac{x_1}{|x|^2} \right)^\top$ where $x = (x_1, x_2)^\top$.

This kernel is used to describe the dynamics of electromagnetism [13].

For the bounded interaction case 1, under Assumption 1, the well-posedness of the SDE (2.1) can be established by applying the interlacing technique to exclude large jumps (defined as exceeding 1) [26, Theorem 4]. For the Biot–Savart interaction case 2, to the best of our knowledge, there is no literature rigorously proving the well-posedness of (2.1). However, we do not focus on this issue in the present paper, and thus omit further discussion. To manage possible singularities in the interaction kernel K , one can consider the regularized form, for instance, for the potential, the modification $K^\varepsilon(x) = \frac{1}{2\pi} \left(-\frac{x_2}{|x|^{2+\varepsilon}}, \frac{x_1}{|x|^{2+\varepsilon}} \right)^\top$ ensures K^ε is bounded for every $\varepsilon > 0$.

2.2. Lévy–Fokker–Planck equation and Lévy score function. The probability flow serves as a crucial link between the forward Kolmogorov equation and the continuity equation for the density function, as illustrated in (1.1). It effectively handles (nonlinear) diffusion processes through an ODE flow framework facilitated by a well-defined score function. In the following, we investigate the counterpart to the conventional diffusion score function for (2.1), which we refer to as the Lévy score function. To identify this score function, we first need to convert the Lévy–Fokker–Planck equation into a continuity equation. Our formulation of the Lévy–Fokker–Planck equation has appeared in our other work [18]. The result is more general than the α stable Lévy process considered in [16, 41], and has no explicit term of the fractional Laplacian. We start from the infinitesimal generator [1, 25] for (2.1):

$$(2.2) \quad \begin{aligned} (\mathcal{L}[\widehat{p}_t]f)(x) &= \sum_{i=1}^d (b_i(x, t) + (K_i * \widehat{p})(x)) (\partial_i f)(x) + \int_{|r| \geq 1} [f(x + G(r, t)) - f(x)] \nu(dr) \\ &+ \int_{|r| < 1} \left[f(x + F(r, t)) - f(x) - \sum_{i=1}^d F_i(x, z) (\partial_i f)(x) \right] \nu(dr) + \frac{1}{2} \sum_{i,j=1}^d \Sigma_{ij}(x, t) (\partial_i \partial_j f)(x), \end{aligned}$$

for each function $f \in C_0^2(\mathbb{R}^d)$ and each point $x \in \mathbb{R}^d$. We apply the Taylor's theorem to $f(x + F(r, t))$ and $f(x + G(r, t))$ at the point x : $f(x + F(r, t)) = f(x) + \sum_{i=1}^d F_i(r, t) \int_0^1 (\partial_i f)(x + \lambda F(r, t)) d\lambda$. Substitute it to (2.2), and compute the adjoint operator of $\mathcal{L}[\widehat{p}_t]$, with more details in [18], we then have the following form of the Lévy-Fokker-Planck equation associated with (2.1):

$$(2.3) \quad \begin{aligned} \frac{\partial \widehat{p}_t(x)}{\partial t} = & - \sum_{i=1}^d \frac{\partial}{\partial x_i} \left[\left(b_i(x, t) + (K_i * \widehat{p}_t)(x) - \int_{|r|<1} F_i(r, t) \nu(dr) \right) \widehat{p}_t(x) \right] \\ & - \int_{|r|<1} \int_0^1 \sum_{i=1}^d \frac{\partial}{\partial x_i} (F_i(r, t) \widehat{p}_t(x - \lambda F(r, t))) d\lambda \nu(dr) \\ & - \int_{|r|\geq 1} \int_0^1 \sum_{i=1}^d \frac{\partial}{\partial x_i} (G_i(r, t) \widehat{p}_t(x - \lambda G(r, t))) d\lambda \nu(dr) + \frac{1}{2} \sum_{i,j=1}^d \frac{\partial^2 (\Sigma_{ij}(x, t) \widehat{p}_t(x))}{\partial x_i \partial x_j}. \end{aligned}$$

which can be rewritten as the *continuity equation*:

$$(2.4) \quad \begin{aligned} \frac{\partial \widehat{p}_t(x)}{\partial t} = & - \sum_{i=1}^d \frac{\partial}{\partial x_i} \left[\left(b_i(x, t) + (K_i * \widehat{p}_t)(x) - \int_{|r|<1} F_i(r, t) \nu(dr) \right. \right. \\ & + \int_{|r|<1} \int_0^1 \frac{F_i(r, t) \widehat{p}_t(x - \lambda F(r, t))}{\widehat{p}_t(x)} d\lambda \nu(dr) + \int_{|r|\geq 1} \int_0^1 \frac{G_i(r, t) \widehat{p}_t(x - \lambda G(r, t))}{\widehat{p}_t(x)} d\lambda \nu(dr) \\ & \left. \left. - \frac{1}{2} \sum_{j=1}^d \frac{\partial}{\partial x_j} \Sigma_{ij}(x, t) - \frac{1}{2} \sum_{j=1}^d \Sigma_{ij}(x, t) \frac{\partial}{\partial x_j} \widehat{p}_t(x) \right) \widehat{p}_t(x) \right] =: -\nabla \cdot (\mathcal{V}[\widehat{p}_t](x, t) \widehat{p}_t(x)). \end{aligned}$$

Based on (2.4), the solution density \widehat{p}_t to the Lévy-Fokker-Planck equation (2.3) can be interpreted as the pushforward of μ_0 under the flow map $X_{s,t}^*$ governed by

$$(2.5) \quad \frac{dX_{s,t}^*(x)}{dt} = \mathcal{V}[\widehat{p}_t](X_{s,t}^*(x), t), \quad X_{s,s}^*(x) = x, \quad t \geq s \geq t_0,$$

referred to as the *probability flow equation*. Here the vector field depends on the \widehat{p}_t in a self-consistent way:

$$(2.6) \quad \begin{aligned} \mathcal{V}[\widehat{p}_t](x, t) := & b(x, t) + (K * \widehat{p}_t)(x) - \int_{|r|<1} F(r, t) \nu(dr) - \frac{\nabla \cdot \Sigma(x, t)}{2} - \sum_{j=1}^d \frac{\Sigma_{ij}(x, t)}{2} \nabla \log \widehat{p}_t(x) \\ & + \int_{|r|<1} \int_0^1 \frac{F(r, t) \widehat{p}_t(x - \lambda F(r, t))}{\widehat{p}_t(x)} d\lambda \nu(dr) + \int_{|r|\geq 1} \int_0^1 \frac{G(r, t) \widehat{p}_t(x - \lambda G(r, t))}{\widehat{p}_t(x)} d\lambda \nu(dr) \\ =: & b(x, t) + (K * \widehat{p}_t)(x) - \int_{|r|<1} F(r, t) \nu(dr) - \frac{1}{2} \nabla \cdot \Sigma(x, t) - \widehat{S}[\widehat{p}_t](x, t). \end{aligned}$$

In the above, we define the *generalized score function* \widehat{S} as follows:

$$(2.7) \quad \widehat{S}[\widehat{p}_t](x, t) := \frac{1}{2} \sum_{j=1}^d \Sigma_{ij}(x, t) \nabla \log \widehat{p}_t(x) + \widehat{S}_L[\widehat{p}_t](x, t)$$

$$(2.8) \quad \begin{aligned} \widehat{S}_L[\widehat{p}_t](x, t) := & - \int_{|r|<1} \int_0^1 \frac{F(r, t) \widehat{p}_t(x - \lambda F(r, t))}{\widehat{p}_t(x)} d\lambda \nu(dr) \\ & - \int_{|r|\geq 1} \int_0^1 \frac{G(r, t) \widehat{p}_t(x - \lambda G(r, t))}{\widehat{p}_t(x)} d\lambda \nu(dr). \end{aligned}$$

The gradient term $\nabla \log \widehat{p}_t$ in \widehat{S} of (2.7) is recognized as the conventional score function derived from the Laplacian terms associated with Gaussian noise, which will be

referred to as **diffusion score**. \widehat{S}_L in (2.8) consist of non-local double integral terms, arising from jump noise, which is called the **Lévy score** function.

2.3. Isotropic α -stable Lévy process. The fractional score function $s_t^{(\alpha)}(x) = ((-\Delta)^{\frac{\alpha-2}{2}} \nabla p_t(x))/p_t(x)$, $\alpha \in (1, 2]$, is proposed in Lévy-type score-based generative modeling [41] and used in [16] to solve the Lévy–Fokker–Planck equation through physics-informed neural networks. This fractional score function is the special case of our result above. Consider the special α -stable Lévy processes: $dX_t = \widehat{b}(X_{t-}, t) dt + \sigma(X_{t-}, t) dB_t + \sigma_L(t) dL_t^\alpha$ which fall within our diffusion-jump SDE (2.1) with $K = 0$, $F(r, t) = G(r, t) = r\sigma_L(t)$, and $\nu(dr)$ is the α -stable Lévy measure $\nu_\alpha(dr) \sim |r|^{-d-\alpha} dr$; note that $\int_{|r|<1} F(r, t)\nu(dr) = 0$. In this special case, the Lévy–Fokker–Planck equation (2.3) reads

$$\begin{aligned} \frac{\partial \widehat{p}_t(x)}{\partial t} &= - \sum_{i=1}^d \frac{\partial [b_i(x, t)\widehat{p}_t(x)]}{\partial x_i} + \sum_{i,j=1}^d \frac{\partial^2 (\Sigma_{ij}(x, t)\widehat{p}_t(x))}{2\partial x_i \partial x_j} + \int_{\mathbb{R}^d \setminus \{0\}} (p(x - \sigma_L(t)r) - p(x)) \nu_\alpha(dr) \\ &= - \sum_{i=1}^d \frac{\partial [b_i(x, t)\widehat{p}_t(x)]}{\partial x_i} + \sum_{i,j=1}^d \frac{\partial^2 (\Sigma_{ij}(x, t)\widehat{p}_t(x))}{2\partial x_i \partial x_j} - \sigma_L^\alpha(t)(-\Delta)^{\frac{\alpha}{2}} \widehat{p}_t(x) \end{aligned}$$

where $(-\Delta)^{\frac{\alpha}{2}}$ denote the fractional Laplacian of order $\frac{\alpha}{2}$ [6], i.e.,

$$(-\Delta)^{\frac{\alpha}{2}} \widehat{p}_t(x) = C_{d,\alpha} \int_{\mathbb{R}^d} \frac{\widehat{p}_t(y) - \widehat{p}_t(x)}{|x-y|^{d+\alpha}} dy,$$

with a normalizing constant $C_{d,\alpha}$. Note that [41, Lemma C.1]

$$(-\Delta)^{\frac{\alpha}{2}} \widehat{p}_t(x) = -\nabla \cdot \left((-\Delta)^{\frac{\alpha-2}{2}} \nabla \widehat{p}_t(x) \right) = -\nabla \cdot (s^{(\alpha)t(x)} \widehat{p}_t(x)).$$

So the Lévy score function we define in (2.8) reduces to the fractional score function $\sigma_L^\alpha(t)s_t^{(\alpha)}(x)$.

2.4. Probability flow for probability density function. The remarkable property of the continuity equation (2.4) is the following: The flow associated with the deterministic ordinary differential equation (2.5) transports the initial distribution μ_0 forward exactly along the density distribution \widehat{p}_t of the SDE (2.1). To turn this idea into a feasible numerical algorithm certainly needs to obtain the generalized score \widehat{S} or the velocity $\mathcal{V}(x, t)$ in (2.6) beforehand, which will be studied in next section. If x is a sample from the initial distribution μ_0 , then $X_{t_0, t}^*(x)$ in (2.5) will be a sample from \widehat{p}_t . We use $\#$ to denote the push-forward operation, then $\widehat{p}_t = X_{t_0, t}^* \# \mu_0$ can be determined at any position using the change of variables formula [31, 40]:

$$(2.9) \quad \widehat{p}_t(x) = \mu_0(X_{t, t_0}^*(x)) \exp \left(- \int_{t_0}^t \nabla \cdot \mathcal{V}[\widehat{p}_t](X_{t, s}^*(x), s) ds \right),$$

where $\nabla \cdot \mathcal{V}$ is the divergence of the velocity field defined in (2.6). It is straightforward to observe that \widehat{p}_t , the solution of the Lévy–Fokker–Planck equation (2.3), is the fixed point of the map $p_t \mapsto \mu_0(X_{t, t_0}^*(x)) \exp \left(- \int_{t_0}^t \nabla \cdot \mathcal{V}[p_t](X_{t, s}^*(x), s) ds \right)$.

By evolving an ensemble of N independent realizations of (2.5), referred to as “particles”, according to

$$(2.10) \quad \frac{dX^{N,i}(t)}{dt} = \mathcal{V}[\widehat{p}_t](X^{N,i}(t), t), \quad i = 1, \dots, N, \quad X^{N,i}(t_0) \sim \mu_0,$$

an empirical approximation to \widehat{p}_t is obtained: $\widehat{p}_t(x) \approx \frac{1}{N} \sum_{i=1}^N \delta_{x-X^{N,i}(t)}$.

3. Score-based Particle Approach: Theoretical and Numerical Analysis. Recall (2.9), the general principle involves here addresses the following fixed-point problem: For any given velocity field $V^{in}(x, t)$, the flow dictated by the ODE (2.5) will transport the initial density μ to obtain p_t , and this transported p_t furthermore induces the new velocity field V^{out} defined via (2.6). It is evident that the true velocity field \mathcal{V} is the fixed point of this map $V^{in} \mapsto V^{out}$. Thus, if we are provided with a set of vector fields $\{f^\theta\}_{\theta \in \Theta}$, and obtain its corresponding probability flows p_t^θ via (2.5), the ideal choice of these vector fields that approximate the true vector field is the one that minimizes the following loss function with some samples from p_t^θ : $\int_{t_0}^T \int_{\Omega} |f^\theta(x, t) - \mathcal{V}[p_t^\theta](x, t)|^2 p_t^\theta(x) dx dt$.

Moving forward, we will first establish a theoretical foundation for our method in Section 3.1 using the above loss function. Following this, we will develop a specific algorithm in Section 3.2 and conduct a detailed error analysis in Section 3.3.

3.1. The Kullback–Leibler divergence error. For simplicity, we introduce the following notations

$$(3.1) \quad \widehat{b}(x, t) := b(x, t) - \int_{|r| < 1} F(r, t) \nu(dr) - \frac{1}{2} \nabla \cdot \Sigma(x, t),$$

$$(3.2) \quad \mathcal{I}_t^{F, G}[\widehat{p}_t](x) := \mathcal{I}_t^F[\widehat{p}_t](x) + \mathcal{I}_t^G[\widehat{p}_t](x),$$

$$(3.3) \quad \mathcal{I}_t^F[\widehat{p}_t](x) := \int_{|r| < 1} \int_0^1 \frac{F(r, t) \widehat{p}_t(x - \lambda F(r, t))}{\widehat{p}_t(x)} d\lambda \nu(dr)$$

$$(3.4) \quad \mathcal{I}_t^G[\widehat{p}_t](x) := \int_{|r| \geq 1} \int_0^1 \frac{G(r, t) \widehat{p}_t(x - \lambda G(r, t))}{\widehat{p}_t(x)} d\lambda \nu(dr).$$

And recall the vector field (2.6), it is written as

$$(3.5) \quad \mathcal{V}[\mu](x, t) := \widehat{b}(x, t) + (K * \mu)(x) - \frac{1}{2} \Sigma(x, t) \nabla \log \mu + \mathcal{I}_t(\mu, F, G).$$

Now suppose we are given a family of time-varying hypothesis velocity fields $\{f^\theta, f^\theta : \mathbb{R}^d \times [t_0, \infty) \rightarrow \mathbb{R}^d\}_{\theta \in \Theta}$ for some index set Θ , and let p_t^θ be the solution to the continuity equation

$$(3.6) \quad \frac{\partial p_t^\theta(x)}{\partial t} = -\nabla \cdot (f^\theta(x, t) p_t^\theta(x)), \quad p_{t_0}^\theta = \mu_0.$$

Similar with previous arguments, the solution density p_t^θ can be viewed as the push forward of μ_0 under the flow map $X_{s, t}^\theta$ of the ordinary differential equation

$$(3.7) \quad \frac{dX_{s, t}^\theta(x)}{dt} = f^\theta(X_{s, t}^\theta(x), t), \quad X_{s, s}^\theta(x) = x, \quad t, s \geq t_0,$$

and thus the density function can be written as

$$(3.8) \quad p_t^\theta(x) = \mu_0(X_{t_0, t}^\theta(x)) \exp\left(-\int_{t_0}^t \nabla \cdot f^\theta(X_{t_0, s}^\theta(x), s) ds\right),$$

as discussed before.

Let us make some assumptions on the the initial distribution μ_0 , the Lévy-Fokker-Planck solution \widehat{p} , and the parametrized vector fields $\{f^\theta\}_{\theta \in \Theta}$. In the remainder of this paper, we will focus on the case where Ω is a torus. The method for extending this to an unbounded domain is similar to the approach detailed in [32, Appendix G], which requires additional assumptions about the regularity of the initial distribution μ_0 and the true probability flow \widehat{p}_t .

ASSUMPTION 2.

1. The initial distribution μ_0 is absolutely continuous with respect to the Lebesgue measure (we still denote its density as μ_0) and there exists a positive constant C_0 such that $(C_0)^{-1} \leq \mu_0(x) \leq C_0$, $\forall x \in \Omega$, and $\mu_0 \in C^2(\Omega)$;
2. For every $T \geq 0$, the solution to (2.3), $\widehat{p}_t \in C^3(\Omega)$ for every $t \geq t_0$ and there is a positive constant C_T^* such that $(C_T^*)^{-1} \leq \widehat{p}_t(x) \leq C_T^*$, $\forall x \in \Omega$, $t \in [t_0, T]$.
3. The velocity field $f^\theta(\cdot, \cdot) \in C^{2,1}(\Omega \times \mathbb{R}, \mathbb{R}^d)$ for every $\theta \in \Theta$. For every $T \geq t_0$, there is a positive constant C_T such that $\sup_{\theta \in \Theta} \sup_{(x,t) \in \Omega \times [t_0, T]} |\nabla \cdot f^\theta(x, t)| \leq C_T$.

Remark 3.1. The Assumption 2-2 can be achieved under some mild conditions. For further details, we refer to [11, 30] as references. Under Assumption 2-3, for every $T \geq t_0$, it is easy to show that there exists a constant C_T^f (dependent on C_T and T only) such that $(C_T^f)^{-1} \leq p_t^\theta(x) \leq C_T^f$, $\forall x \in \Omega$, $t \in [t_0, T]$, $\theta \in \Theta$.

We now give an upper bound for the KL divergence between p^θ and \widehat{p} for bounded kernel case 1 and Biot–Savart kernel case 2.

THEOREM 3.2. *For interaction kernels 1 (bounded) and 2 (Biot-Savart), let $p_t^\theta(x)$ denote the solution to the transport equation (3.6), and let $\widehat{p}_t(x)$ denote the solution to the Lévy–Fokker–Planck equation (2.3). Suppose Assumption 1 and 2 hold, then*

$$\sup_{t \in [t_0, T]} D_{\text{KL}}(p_t^\theta \| \widehat{p}_t) \leq 3 \exp(\bar{C}T) C_\sigma \int_{t_0}^t \int_{\Omega} |f^\theta(x, t) - \mathcal{V}[p_t^\theta](x, t)|^2 p_t^\theta(x) dx dt,$$

where \bar{C} is a constant given in (3.16).

3.2. Sequential Lévy score-based particle method. By Theorem 3.2, we can minimize the following function to control the KL divergence between the numerical p_t^θ and the true \widehat{p}_t : $\min_{\theta} \int_{t_0}^T \int_{\Omega} |f^\theta(x, t) - \mathcal{V}[p_t^\theta](x, t)|^2 p_t^\theta(x) dx dt$, where \mathcal{V} is defined in (3.5). By (2.5) and (2.6), the velocity field f^θ is given by

$$(3.10) \quad f^\theta(x, t) = b(x, t) - \int_{|r| < 1} F(r, t) \nu(dr) - \frac{1}{2} \nabla \cdot \Sigma(x, t) - s^\theta(x, t),$$

where s^θ is the numerical score function parametrized by θ ,

$$(3.11) \quad s^\theta \approx \widehat{S}[\widehat{p}_t] - K * \widehat{p}_t.$$

Now the optimization problem turns to

$$(3.12) \quad \begin{aligned} & \min_{\theta \in \Theta} \int_{t_0}^T \int_{\Omega} |f^\theta(x, t) - \mathcal{V}[p_t^\theta](x, t)|^2 p_t^\theta(x) dx dt \\ &= \min_{\theta \in \Theta} \int_{t_0}^T \int_{\Omega} \left| s^\theta(x, t) + \left(K * p_t^\theta \right)(x) - \frac{1}{2} \Sigma(x, t) \nabla \log p_t^\theta(x) + \mathcal{I}_t^{F, G}[p_t^\theta](x) \right|^2 p_t^\theta(x) dx dt. \end{aligned}$$

The primary difficulty with this optimization problem (3.12) is that p_t^θ depends on s^θ , since the velocity f^θ used in (3.6) depends on s^θ . Such an issue has been observed in [4]. To make the resulting minimization of the right-hand side of (3.9) practical, we consider to learn $s^\theta(x, t)$ separately at each time sub-interval in a time-discrete way so that p_t^θ can be assumed unchanged within each short time sub-interval.

Then we consider the loss at any given time $t \in [t_0, T]$, by assuming p_t^θ is frozen:

$$\begin{aligned}
& \int_{\Omega} \left| f^\theta(x, t) - \mathcal{V}[p_t^\theta](x, t) \right|^2 p_t^\theta(x) \, dx \\
&= \int_{\Omega} \left| s^\theta(x, t) + \left(K * p_t^\theta \right)(x) - \frac{1}{2} \Sigma(x, t) \nabla \log p_t^\theta(x) + \mathcal{I}_t^{F,G}[p_t^\theta](x) \right|^2 p_t^\theta(x) \, dx \\
&= \int_{\Omega} \left| s^\theta(x, t) \right|^2 p_t^\theta(x) \, dx + \int_{\Omega} \left| \left(K * p_t^\theta \right)(x) - \frac{1}{2} \Sigma(x, t) \nabla \log p_t^\theta(x) + \mathcal{I}_t^{F,G}[p_t^\theta](x) \right|^2 \\
&\quad \times p_t^\theta(x) \, dx + 2 \int_{\Omega} s^\theta(x, t) \cdot \left[\left(K * p_t^\theta \right)(x) - \frac{1}{2} \Sigma(x, t) \nabla \log p_t^\theta(x) + \mathcal{I}_t^{F,G}[p_t^\theta](x) \right] p_t^\theta(x) \, dx.
\end{aligned}$$

Note that the second term contains no s^θ , so we can drop it during the optimization procedure. For the remaining first and third terms, we shall express them by the expectation w.r.t. p_t^θ . That is, $\int_{\Omega} \left| s^\theta(x, t) \right|^2 p_t^\theta(x) \, dx = \mathbb{E}_{X_t \sim p_t^\theta} \left| s^\theta(X_t, t) \right|^2$, and $\int_{\Omega} s^\theta(x, t) \cdot \left(K * p_t^\theta \right)(x) p_t^\theta(x) \, dx = \mathbb{E}_{X_t \sim p_t^\theta} \mathbb{E}_{\tilde{X}_t \sim p_t^\theta} \left(s^\theta(X_t, t) \cdot K(X_t - \tilde{X}_t) \right)$. And by integral by part, $\int_{\Omega} s^\theta(x, t) \cdot \left[-\frac{1}{2} \Sigma(x, t) \nabla \log p_t^\theta(x) \right] p_t^\theta(x) \, dx = -\frac{1}{2} \int_{\Omega} \left[\Sigma(x, t) s^\theta(x, t) \right] \cdot \nabla p_t^\theta(x) \, dx = \frac{1}{2} \mathbb{E}_{X_t \sim p_t^\theta} \left[\nabla \cdot \left(\Sigma(X_t, t) s^\theta(X_t, t) \right) \right]$. And for the non-local terms by (3.1) we have,

$$\begin{aligned}
& \int_{\Omega} s^\theta(x, t) \mathcal{I}_t^{F,G}[p_t^\theta](x) p_t^\theta(x) \, dx = \int_{\Omega} s^\theta(x, t) \cdot \int_{|r| < 1} F(r, t) \int_0^1 p_t^\theta(x - \lambda F(r, t)) \\
&\quad \times d\lambda \nu(dr) \, dx + \int_{\Omega} s^\theta(x, t) \cdot \int_{|r| \geq 1} G(r, t) \int_0^1 p_t^\theta(x - \lambda G(r, t)) d\lambda \nu(dr) \, dx \\
&= \mathbb{E}_{X_t \sim p_t^\theta} \left(\int_{|r| < 1} \int_0^1 \left(s^\theta(X_t + \lambda F(r, t), t) \cdot F(r, t) \right) d\lambda \nu(dr) \right) \\
&\quad + \mathbb{E}_{X_t \sim p_t^\theta} \left(\int_{|r| \geq 1} \int_0^1 \left(s^\theta(X_t + \lambda G(r, t), t) \cdot G(r, t) \right) d\lambda \nu(dr) \right).
\end{aligned}$$

In summary, we have the following loss function for the function $s^\theta(\cdot, t)$ at time t as (3.13)

$$\begin{aligned}
Loss(t) &= \mathbb{E}_{X_t \sim p_t^\theta} \left(\left| s^\theta(X_t, t) \right|^2 \right) + \mathbb{E}_{X_t \sim p_t^\theta} \left[\nabla \cdot \left(\Sigma(X_t, t) s^\theta(X_t, t) \right) \right] + 2 \mathbb{E}_{X_t \sim p_t^\theta} \left[\right. \\
&\mathbb{E}_{X'_t \sim p_t^\theta} \left(s^\theta(X_t, t) \cdot K(X_t - X'_t) \right) \left. \right] + 2 \mathbb{E}_{X_t \sim p_t^\theta} \left(\int_{|r| < 1} \int_0^1 s^\theta(X_t + \lambda F(r, t), t) \cdot F(r, t) \right. \\
&\quad \left. \times d\lambda \nu(dr) \right) + 2 \mathbb{E}_{X_t \sim p_t^\theta} \left(\int_{|r| \geq 1} \int_0^1 s^\theta(X_t + \lambda G(r, t), t) \cdot G(r, t) d\lambda \nu(dr) \right).
\end{aligned}$$

Given the current samples of X_t from law p_t^θ at any time t , we can obtain $s^\theta(\cdot, t)$ via direct minimization of objective in (3.13). Given $s^\theta(\cdot, t)$, we propagate $X_{t_0, t}^\theta$ forward in time up to time $t + \Delta t$ via (3.7). The resulting procedure, which alternates between self-consistent score estimation and sample propagation, is presented in Algorithm 3.1 for the choice of a forward-Euler integration routine as t to $t + \Delta t$.

Here the one dimensional integral of $\int_0^1 \bullet d\lambda$ is discretized by any quadrature scheme, like the trapezoidal rule. The integral w.r.t. $\nu(dr)$ in \mathbb{R}^d is approximated by the quadrature scheme in low dimension or by the Monte Carlo average in high dimension. $\int_{|r| < 1} F(r, t) \nu(dr)$ is pre-computed as a function of t only.

Algorithm 3.1 Sequential Lévy score-based transport modeling to solve (2.1)

Input: An initial time t_0 . A set of N samples $\{x^{(i)}\}_{i=1}^N$ from the initial distribution p_{t_0} . A time step Δt and the number of steps N_T . Initialize sample locations $X_{t_0}^{(i)} = x^{(i)}$ for $i = 1, \dots, N$.

for $k = 0 : N_T$ **do**

Optimize (3.13):

$$s(\cdot, t_k) = \underset{s(\cdot, t_k)}{\operatorname{argmin}} \frac{1}{N} \sum_{i=1}^N \left[\left| s(X_{t_k}^{(i)}, t_k) \right|^2 + 2 \left(\frac{1}{N} \sum_{j=1}^N s(X_{t_k}^{(i)}, t_k) K(X_{t_k}^{(i)} - X_{t_k}^{(j)}) \right) \right. \\ \left. + \nabla \cdot \left(\Sigma(X_{t_k}^{(i)}, t_k) s(X_{t_k}^{(i)}, t_k) \right) + 2 \int_{|r| < 1} \int_0^1 s(X_{t_k}^{(i)} + \lambda F(r, t_k), t_k) + \lambda F(r, t_k), t_k) \cdot F(r, t_k) d\lambda \nu(dr) \right. \\ \left. + 2 \int_{|r| \geq 1} \int_0^1 s(X_{t_k}^{(i)} + \lambda G(r, t_k), t_k) \cdot G(r, t_k) d\lambda \nu(dr) \right];$$

Propagate the samples for $i = 1, \dots, N$:

$$X_{t_{k+1}}^{(i)} = X_{t_k}^{(i)} + \Delta t \left[b(X_{t_k}^{(i)}, t_k) - \int_{|r| < 1} F(r, t) \nu(dr) - \frac{1}{2} \nabla \cdot \Sigma(X_{t_k}^{(i)}, t_k) - s(X_{t_k}^{(i)}, t_k) \right];$$

Set $t_{k+1} = t_k + \Delta t$;

end for

return

Output: Samples $\{X_{t_k}^{(i)}\}_{i=1}^N$ from p_{t_k} and $\{s(X_{t_k}^{(i)}, t_k)\}_{i=1}^N$ for all $\{t_k\}_{k=0}^{N_T}$.

Remark 3.3. Algorithm 3.1 trains neural networks to approximate the sum of the Lévy score function and the negative interaction term. So, the probability flow in Algorithm 3.1 can evolve the N particles independently without any interaction. This approach contrasts with the one described in [28], which did not include the score contribution from the interaction term. The extra cost here is the double sum of $\sum_i \sum_j$ in the loss function for the score training, but since the training process is based on the mini-batch, the random batch method of randomly selecting $m \ll N$ particles is easily applied here for this double sum.

If the initial density \hat{p}_0 has the analytical expression like the Gaussian distribution, then the initial score function $s^\theta(\cdot, t_0)$ is computed by the direct minimization of the following loss due to (3.11):

$$\frac{\int_{\Omega} \left\| s(\cdot, t_0) - \widehat{S}[\hat{p}_0](x, t_0) + K * \hat{p}_0(x) \right\|^2 \hat{p}_0(x) dx}{\int_{\Omega} \left\| \widehat{S}[\hat{p}_0](x, t_0) - K * \hat{p}_0(x) \right\|^2 \hat{p}_0(x) dx} \approx \frac{\sum_{i=1}^N \left\| s(X_0^{(i)}, t_0) - \widehat{S}[\hat{p}_0](X_0^{(i)}, t_0) + K * \hat{p}_0(x) \right\|^2}{\sum_{i=1}^N \left\| \widehat{S}[\hat{p}_0](X_0^{(i)}, t_0) - K * \hat{p}_0(x) \right\|^2},$$

where $\widehat{S}[\hat{p}_0]$ is defined in (2.7).

3.3. Error analysis of Algorithm 3.1. Now we focus on analyzing the discrete error associated with Algorithm 3.1. The following theorem demonstrates that the discrete numerical error of Algorithm 3.1 is on the order of $1/\sqrt{N}$, where N represents the number of particles utilized in the algorithm.

THEOREM 3.4. *Let N , N_T , Δt , t_0 and p_{t_0} be defined as in Algorithm 3.1 and denote $\varepsilon := \sup_{x \in \Omega, t_0 \leq t \leq N_T \Delta t} \left| s(x, t) + (K * \hat{p}_t)(x) - \frac{\Sigma(x, t)}{2} \nabla \log \hat{p}_t(x) + \mathcal{I}_t^{F, G}[\hat{p}_t](x) \right|$, as the approximation error of a neural network function $s(x, t)$, with \hat{p}_t the solution of the Lévy-Fokker-Planck equation (2.3). Denote $X_{t_0, t}^N(x)$ the numerical transport map obtained from Algorithm 3.1 by stacking the transport map in each sub-interval starting from x . Let $X_{t_0, t}^*$ starting from x solve the deterministic probability flow equation $\frac{d}{dt} X_{t_0, t}^*(x) = \mathcal{V}[\hat{p}_t](X_{t_0, t}^*(x), t) = \widehat{b}(X_{t_0, t}^*(x), t) + (K * \hat{p}_t)(X_{t_0, t}^*(x)) - \frac{1}{2} \Sigma(X_{t_0, t}^*(x), t) \nabla \log \hat{p}_t(X_{t_0, t}^*(x)) + \mathcal{I}_t^{F, G}[\hat{p}_t](X_{t_0, t}^*(x), t)$, corresponding to ODE (2.10),*

\widehat{b} and $\mathcal{I}_t^{F,G}[\widehat{p}_t]$ are given in (3.1), (3.2). Under Assumption 2, for any $t \in \{t_0 + n\Delta t\}_{n=0}^{N_T}$,

$$(3.14) \quad \mathbb{E}_{x \sim p_{t_0}} \left| X_{t_0,t}^*(x) - X_{t_0,t}^N(x) \right| \leq \left[\mathcal{O}\left(\frac{1}{\sqrt{N}}\right) + \mathcal{O}(\varepsilon) + \mathcal{O}(\Delta t) \right] (t - t_0),$$

as $\frac{1}{N}$, ε and Δt all tend to 0.

3.4. Proof of Theorem 3.2. We first present a lemma about the bounds of the squared L^2 -norm of two probability density functions by their KL divergence, which will be used in our main proof.

LEMMA 3.5. *Suppose p and q are two probability densities on Ω , and there exists a positive constant τ such that $0 < p(x), q(x) < \tau$, $\forall x \in \Omega$. Then we have*

$$\int_{\Omega} |p(x) - q(x)|^2 dx \leq \frac{2\tau}{1 - \log 2} D_{\text{KL}}(p||q).$$

Proof. Define $\zeta(x) := \frac{q(x)-p(x)}{p(x)}$, $\forall x \in \Omega$. Then $D_{\text{KL}}(p||q) = \int_{\Omega} p(x) \log \frac{p(x)}{q(x)} dx = -\int_{\Omega} p(x) \log(1 + \zeta(x)) dx$. Define two Borel sets as follows, $A := \{x|\zeta(x) > 1\} = \{x|q(x) > 2p(x)\}$, $B := \{x|\zeta(x) \leq 1\} = \{x|q(x) \leq 2p(x)\}$. We obtain that for $x \in A$, $1 + \zeta(x) \leq e^{\alpha\zeta(x)}$ where $\alpha = \log 2$; for $x \in B$, $1 + \zeta(x) \leq e^{\zeta(x) - \beta\zeta(x)^2}$ where $\beta = 1 - \log 2$. Note that p and q are two probabilities density on Ω , that is $\int_{\Omega} p(x)\zeta(x) dx = \int_{\Omega} (q(x) - p(x)) dx = 0$, which implies that $\int_A p(x)\zeta(x) dx = -\int_B p(x)\zeta(x) dx$. Thus

$$\begin{aligned} D_{\text{KL}}(p||q) &= -\int_A p(x) \log(1 + \zeta(x)) dx - \int_B p(x) \log(1 + \zeta(x)) dx \\ &\geq -\alpha \int_A p(x)\zeta(x) dx - \int_B p(x)\zeta(x) dx + \beta \int_B p(x)\zeta(x)^2 dx \\ &= (1 - \alpha) \int_A p(x)\zeta(x) dx + \beta \int_{\Omega} p(x)\zeta(x)^2 dx \\ &= (1 - \log 2) \left(\int_A |q(x) - p(x)| dx + \int_B p(x) \left(\frac{q(x) - p(x)}{p(x)} \right)^2 dx \right). \end{aligned}$$

For the first term in right hand side of the above equality, we have $\int_A |q(x) - p(x)| dx \geq \frac{1}{2\tau} \int_A |q(x) - p(x)|^2 dx$. For the second term, we have $\int_B p(x) \left(\frac{q(x) - p(x)}{p(x)} \right)^2 dx \geq \frac{1}{2\tau} \int_B |q(x) - p(x)|^2 dx$. Finally, we have $D_{\text{KL}}(p||q) \geq \frac{1 - \log 2}{2\tau} \int_{\Omega} |q(x) - p(x)|^2 dx$. \square

Proof of Theorem 3.2. The proof is inspired by the methodologies presented in [4, Proposition 1] and [32, Appendix E]. However, dealing with the Lévy term introduces substantial complexity, requiring the introduction of novel techniques for a thorough analysis.

Firstly, according to the definition of KL divergence, we derive that

$$\begin{aligned}
\frac{d}{dt} D_{\text{KL}}(p_t^\theta \| \widehat{p}_t) &= \frac{d}{dt} \int_{\Omega} \log \left(\frac{p_t^\theta(x)}{\widehat{p}_t(x)} \right) p_t^\theta(x) dx \\
&= - \int_{\Omega} \frac{p_t^\theta(x)}{\widehat{p}_t(x)} \partial_t \widehat{p}_t(x) dx + \int_{\Omega} \log \left(\frac{p_t^\theta(x)}{\widehat{p}_t(x)} \right) \partial_t p_t^\theta(x) dx + \int_{\Omega} \partial_t p_t^\theta(x) dx \\
&= - \int_{\Omega} \frac{p_t^\theta(x)}{\widehat{p}_t(x)} \partial_t \widehat{p}_t(x) dx + \int_{\Omega} \log \left(\frac{p_t^\theta(x)}{\widehat{p}_t(x)} \right) \partial_t p_t^\theta(x) dx \\
&= - \int_{\Omega} \mathcal{V}[\widehat{p}_t](x, t) \cdot \nabla \left(\frac{p_t^\theta(x)}{\widehat{p}_t(x)} \right) \widehat{p}_t(x) dx + \int_{\Omega} f^\theta(x, t) \cdot \nabla \log \left(\frac{p_t^\theta(x)}{\widehat{p}_t(x)} \right) p_t^\theta(x) dx \\
&= - \int_{\Omega} \left(\mathcal{V}[\widehat{p}_t](x, t) - f^\theta(x, t) + \mathcal{V}[p_t^\theta](x, t) - \mathcal{V}[p_t^\theta](x, t) \right) \cdot \nabla \log \left(\frac{p_t^\theta(x)}{\widehat{p}_t(x)} \right) p_t^\theta(x) dx,
\end{aligned}$$

where we used $\int \partial_t p_t^\theta(x) dx = 0$ and the integration by parts.

With the expression $\mathcal{V}[p_t^\theta]$ of (3.1), we decompose the derivative of the KL divergence as follows,

$$\begin{aligned}
\frac{d}{dt} D_{\text{KL}}(p_t^\theta \| \widehat{p}_t) &= \underbrace{\int_{\Omega} \left(f^\theta(x, t) - \mathcal{V}[p_t^\theta](x, t) \right) \cdot \nabla \log \left(\frac{p_t^\theta(x)}{\widehat{p}_t(x)} \right) p_t^\theta(x) dx}_{\text{Perturbation}} \\
&+ \underbrace{\int_{\Omega} \left(\int_{\Omega} K(x-y)(p_t^\theta(y) - \widehat{p}_t(y)) dy \right) \cdot \nabla \log \left(\frac{p_t^\theta(x)}{\widehat{p}_t(x)} \right) p_t^\theta(x) dx}_{\text{Interaction}} \\
&- \underbrace{\int_{\Omega} \frac{1}{2} \left| \nabla \log \left(\frac{p_t^\theta(x)}{\widehat{p}_t(x)} \right) \right|_{\Sigma(x,t)}^2 p_t^\theta(x) dx}_{\text{Diffusion}} \\
&+ \underbrace{\int_{\Omega} \left(\mathcal{I}_t(p_t^\theta, F, G)(x) - \mathcal{I}_t(\widehat{p}_t, F, G)(x) \right) \cdot \nabla \log \left(\frac{p_t^\theta(x)}{\widehat{p}_t(x)} \right) p_t^\theta(x) dx}_{\text{Lévy}},
\end{aligned}$$

where $|\cdot|_{\Sigma(x,t)} = \langle \cdot, \Sigma(x,t) \cdot \rangle$. The bounds for these four terms are studied below respectively in four steps.

(Step 1.) For the perturbation part, by the Cauchy–Schwarz inequality we have

$$\begin{aligned}
&\int_{\Omega} \left(f^\theta(x, t) - \mathcal{V}[p_t^\theta](x, t) \right) \cdot \nabla \log \left(\frac{p_t^\theta(x)}{\widehat{p}_t(x)} \right) p_t^\theta(x) dx \\
&\leq \frac{1}{12C_\sigma} \int_{\Omega} \left| \nabla \log \left(\frac{p_t^\theta(x)}{\widehat{p}_t(x)} \right) \right|^2 p_t^\theta(x) dx + 3C_\sigma \int_{\Omega} \left| f^\theta(x, t) - \mathcal{V}[p_t^\theta](x, t) \right|^2 p_t^\theta(x) dx.
\end{aligned}$$

(Step 2.) For the interaction part, there are two cases 1 and 2 for the interaction kernel K . We discuss each case respectively.

(Bounded interaction) By the Cauchy–Schwarz inequality we have

$$\begin{aligned}
& \int_{\Omega} \left(\int_{\Omega} K(x-y)(p_t^\theta(y) - \widehat{p}_t(y)) dy \right) \cdot \nabla \log \left(\frac{p_t^\theta(x)}{\widehat{p}_t(x)} \right) p_t^\theta(x) dx \\
& \leq \frac{1}{12C_\sigma} \int_{\Omega} \left| \nabla \log \left(\frac{p_t^\theta(x)}{\widehat{p}_t(x)} \right) \right|^2 p_t^\theta(x) dx + 3C_\sigma \int_{\Omega} \left| (K * (p_t^\theta - \widehat{p}_t))(x) \right|^2 p_t^\theta(x) dx \\
& \leq \frac{1}{12C_\sigma} \int_{\Omega} \left| \nabla \log \left(\frac{p_t^\theta(x)}{\widehat{p}_t(x)} \right) \right|^2 p_t^\theta(x) dx + 3C_\sigma (C_K)^2 \left(\int_{\Omega} |p_t^\theta(y) - \widehat{p}_t(y)| dy \right)^2 \\
& \leq \frac{1}{12C_\sigma} \int_{\Omega} \left| \nabla \log \left(\frac{p_t^\theta(x)}{\widehat{p}_t(x)} \right) \right|^2 p_t^\theta(x) dx + 6C_\sigma (C_K)^2 D_{\text{KL}}(p_t^\theta \| \widehat{p}_t),
\end{aligned}$$

where we use the Csiszár–Kullback–Pinsker inequality [40] for the last inequality.

(Biot–Savart interaction) For the Biot–Savart interaction kernel, as noted by [21], it can be written as:

$$K^\top = \nabla \cdot U \quad \text{with} \quad U(x) = \frac{1}{2\pi} \begin{pmatrix} -\arctan\left(\frac{x_1}{x_2}\right) & 0 \\ 0 & \arctan\left(\frac{x_2}{x_1}\right) \end{pmatrix}.$$

We follow the statement in [32, Appendix E.1] to have

$$\begin{aligned}
& \int_{\Omega} \left(\int_{\Omega} K(x-y)(p_t^\theta(y) - \widehat{p}_t(y)) dy \right) \cdot \nabla \log \left(\frac{p_t^\theta(x)}{\widehat{p}_t(x)} \right) p_t^\theta(x) dx \\
& \leq \frac{1}{12C_\sigma} \int_{\Omega} \left| \nabla \log \left(\frac{p_t^\theta(x)}{\widehat{p}_t(x)} \right) \right|^2 p_t^\theta(x) dx + 3C_\sigma \int_{\Omega} \left| (\nabla \log \widehat{p}_t(x))^\top U * (p_t^\theta - \widehat{p}_t)(x) \right|^2 p_t^\theta(x) dx \\
& \quad + 4\|U\|_\infty \left\| \frac{\nabla^2 \widehat{p}_t}{\widehat{p}_t} \right\|_\infty D_{\text{KL}}(p_t^\theta \| \widehat{p}_t) \\
& \leq \frac{1}{12C_\sigma} \int_{\Omega} \left| \nabla \log \left(\frac{p_t^\theta(x)}{\widehat{p}_t(x)} \right) \right|^2 p_t^\theta(x) dx + 3C_\sigma \|\nabla \log \widehat{p}_t\|_\infty^2 \|U\|_\infty^2 \left(\int_{\Omega} |p_t^\theta - \widehat{p}_t|(x) dx \right)^2 \\
& \quad + 4\|U\|_\infty \left\| \frac{\nabla^2 \widehat{p}_t}{\widehat{p}_t} \right\|_\infty D_{\text{KL}}(p_t^\theta \| \widehat{p}_t) \\
& \leq \frac{1}{12C_\sigma} \int_{\Omega} \left| \nabla \log \left(\frac{p_t^\theta(x)}{\widehat{p}_t(x)} \right) \right|^2 p_t^\theta(x) dx \\
& \quad + \left(6C_\sigma \|\nabla \log \widehat{p}_t\|_\infty^2 \|U\|_\infty^2 + 4\|U\|_\infty \left\| \frac{\nabla^2 \widehat{p}_t}{\widehat{p}_t} \right\|_\infty \right) D_{\text{KL}}(p_t^\theta \| \widehat{p}_t),
\end{aligned}$$

we use the Csiszár–Kullback–Pinsker inequality to obtain the last inequality.

(Step 3.) For the Diffusion part, due to Assumption 1-1 we simply have that

$$-\int_{\Omega} \frac{1}{2} \left| \nabla \log \left(\frac{p_t^\theta(x)}{\widehat{p}_t(x)} \right) \right|_{\Sigma(x,t)}^2 p_t^\theta(x) dx \leq -\int_{\Omega} \frac{1}{2C_\sigma} \left| \nabla \log \left(\frac{p_t^\theta(x)}{\widehat{p}_t(x)} \right) \right|^2 p_t^\theta(x) dx.$$

(Step 4.) The last part is about the Lévy terms \mathcal{I} . We have the following

estimate:

$$\begin{aligned}
& \int_{\Omega} \left(\mathcal{I}_t^F [p_t^\theta](x) - \mathcal{I}_t^F [\widehat{p}_t](x) \right) \cdot \nabla \log \left(\frac{p_t^\theta(x)}{\widehat{p}_t(x)} \right) p_t^\theta(x) \, dx \\
& \leq \int_{\Omega} \int_{|r|<1} \int_0^1 \left| \frac{F(r,t)}{p_t^\theta(x)\widehat{p}_t(x)} \right| \left| p_t^\theta(x - \lambda F(r,t))\widehat{p}_t(x) - p_t^\theta(x - \lambda F(r,t))p_t^\theta(x) \right. \\
& \quad \left. + p_t^\theta(x - \lambda F(r,t))p_t^\theta(x) - \widehat{p}_t(x - \lambda F(r,t))p_t^\theta(x) \right| d\lambda \nu(dr) \left| \nabla \log \left(\frac{p_t^\theta(x)}{\widehat{p}_t(x)} \right) \right| p_t^\theta(x) \, dx \\
& \leq \int_{\Omega} \int_{|r|<1} \int_0^1 \left| \frac{F(r,t)p_t^\theta(x - \lambda F(r,t))}{p_t^\theta(x)\widehat{p}_t(x)} \right| \left| \widehat{p}_t(x) - p_t^\theta(x) \right| d\lambda \nu(dr) \left| \nabla \log \left(\frac{p_t^\theta(x)}{\widehat{p}_t(x)} \right) \right| p_t^\theta(x) \, dx \\
& \quad + \int_{\Omega} \left(\int_{|r|<1} \int_0^1 \left| \frac{F(r,t)p_t^\theta(x)}{p_t^\theta(x)\widehat{p}_t(x)} \right| \left| p_t^\theta(x - \lambda F(r,t)) - \widehat{p}_t(x - \lambda F(r,t)) \right| d\lambda \nu(dr) \right) \left| \nabla \log \left(\frac{p_t^\theta(x)}{\widehat{p}_t(x)} \right) \right| p_t^\theta(x) \, dx \\
& \stackrel{(1)}{\leq} 6C_\sigma \int_{\Omega} \left(\int_{|r|<1} \int_0^1 \left| \frac{F(r,t)p_t^\theta(x - \lambda F(r,t))}{p_t^\theta(x)\widehat{p}_t(x)} \right| \left| \widehat{p}_t(x) - p_t^\theta(x) \right| d\lambda \nu(dr) \right)^2 p_t^\theta(x) \, dx \\
& \quad + \frac{1}{12C_\sigma} \int_{\Omega} \left| \nabla \log \left(\frac{p_t^\theta(x)}{\widehat{p}_t(x)} \right) \right|^2 p_t^\theta(x) \, dx \\
& \quad + 6C_\sigma \int_{\Omega} \left(\int_{|r|<1} \int_0^1 \left| \frac{F(r,t)}{\widehat{p}_t(x)} \right| \left| p_t^\theta(x - \lambda F(r,t)) - \widehat{p}_t(x - \lambda F(r,t)) \right| d\lambda \nu(dr) \right)^2 p_t^\theta(x) \, dx \\
& \stackrel{(2)}{\leq} 6C_\sigma (C_T^f)^3 (C_T^*)^2 \int_{|r|<1} |F(r,t)|^2 \nu(dr) \int_{\Omega} \left| \widehat{p}_t(x) - p_t^\theta(x) \right|^2 dx + \frac{1}{12C_\sigma} \int_{\Omega} \left| \nabla \log \left(\frac{p_t^\theta(x)}{\widehat{p}_t(x)} \right) \right|^2 p_t^\theta(x) \, dx \\
& \quad + 6C_\sigma C_T^f (C_T^*)^2 \int_{|r|<1} \int_0^1 |F(r,t)|^2 \int_{\Omega} \left| p_t^\theta(x - \lambda F(r,t)) - \widehat{p}_t(x - \lambda F(r,t)) \right|^2 dx d\lambda \nu(dr) \\
& = 6C_\sigma \left((C_T^f)^3 (C_T^*)^2 + C_T^f (C_T^*)^2 \right) \int_{|r|<1} |F(r,t)|^2 \nu(dr) \int_{\Omega} \left| \widehat{p}_t(x) - p_t^\theta(x) \right|^2 dx + \frac{1}{12C_\sigma} \int_{\Omega} \left| \nabla \log \left(\frac{p_t^\theta(x)}{\widehat{p}_t(x)} \right) \right|^2 p_t^\theta(x) \, dx,
\end{aligned}$$

where the inequality “ $\stackrel{(1)}{\leq}$ ” arises from the Cauchy–Schwarz inequality, and “ $\stackrel{(2)}{\leq}$ ” comes from Assumption 2-2. C_T^f is the constant given in Remark 3.1. Similarly, we have

$$\begin{aligned}
& \int_{\Omega} \left(\mathcal{I}_t^G [p_t^\theta](x) - \mathcal{I}_t^G [\widehat{p}_t](x) \right) \cdot \nabla \log \left(\frac{p_t^\theta(x)}{\widehat{p}_t(x)} \right) p_t^\theta(x) \, dx \\
& \leq 6C_\sigma \left((C_T^f)^3 (C_T^*)^2 + C_T^f (C_T^*)^2 \right) \int_{|r|\geq 1} |G(r,t)|^2 \nu(dr) \int_{\Omega} \left| \widehat{p}_t(x) - p_t^\theta(x) \right|^2 dx \\
& \quad + \frac{1}{12C_\sigma} \int_{\Omega} \left| \nabla \log \left(\frac{p_t^\theta(x)}{\widehat{p}_t(x)} \right) \right|^2 p_t^\theta(x) \, dx.
\end{aligned}$$

By Lemma 3.5, the squared L^2 -norm of $p_t^\theta - \widehat{p}_t$ can be controlled by the KL divergence between p_t^θ and \widehat{p}_t , thus we know that for any $t \in [t_0, T]$,

$$\begin{aligned}
& \int_{\Omega} \left(\mathcal{I}_t^{F,G} [p_t^\theta](x) - \mathcal{I}_t^{F,G} [\widehat{p}_t](x) \right) \cdot \nabla \log \left(\frac{p_t^\theta(x)}{\widehat{p}_t(x)} \right) p_t^\theta(x) \, dx \\
& \leq \frac{1}{6C_\sigma} \int_{\Omega} \left| \nabla \log \left(\frac{p_t^\theta(x)}{\widehat{p}_t(x)} \right) \right|^2 p_t^\theta(x) \, dx + 6C_\sigma C_T^{\text{NG}} D_{\text{KL}}(p_t^\theta \| \widehat{p}_t),
\end{aligned}$$

where

$$(3.15) \quad C_T^{\text{NG}} = \frac{2 \left(C_T^f \wedge C_T^* \right) \left(C_T^f C_T^* \right)^2}{1 - \log 2} \left[\int_{|r|<1} |F(r,t)|^2 \nu(dr) + \int_{|r|\geq 1} |G(r,t)|^2 \nu(dr) \right],$$

Finally, we aggregate the above four bounds to get the upper bound for the

derivative of the KL divergence between p_t^θ and \widehat{p}_t . It is treated for two cases of interaction kernels as below.

(Bounded interaction)

$$\begin{aligned} \frac{d}{dt} D_{\text{KL}}(p_t^\theta \| \widehat{p}_t) &\leq -\frac{1}{6C_\sigma} \int_{\Omega} \left| \nabla \log \left(\frac{p_t^\theta(x)}{\widehat{p}_t(x)} \right) \right|^2 p_t^\theta(x) dx + 6C_\sigma (C_K)^2 D_{\text{KL}}(p_t^\theta \| \widehat{p}_t) \\ &\quad + 3C_\sigma C_T^{\text{nG}} D_{\text{KL}}(p_t^\theta \| \widehat{p}_t) + 3C_\sigma \int_{\Omega} \left| f^\theta(x, t) - \mathcal{V}[p_t^\theta](x, t) \right|^2 p_t^\theta(x) dx \\ &\leq 3 \left(2C_\sigma (C_K)^2 + C_\sigma C_T^{\text{nG}} \right) D_{\text{KL}}(p_t^\theta \| \widehat{p}_t) + 3C_\sigma \int_{\Omega} \left| f^\theta(x, t) - \mathcal{V}[p_t^\theta](x, t) \right|^2 p_t^\theta(x) dx. \end{aligned}$$

(Biot–Savart interaction)

$$\begin{aligned} \frac{d}{dt} D_{\text{KL}}(p_t^\theta \| \widehat{p}_t) &\leq -\frac{1}{6C_\sigma} \int_{\Omega} \left| \nabla \log \left(\frac{p_t^\theta(x)}{\widehat{p}_t(x)} \right) \right|^2 p_t^\theta(x) dx + \left(6C_\sigma \|\nabla \log \widehat{p}_t\|_\infty^2 \|U\|_\infty^2 \right. \\ &\quad \left. + 4\|U\|_\infty \left\| \frac{\nabla^2 \widehat{p}_t}{\widehat{p}_t} \right\|_\infty \right) D_{\text{KL}}(p_t^\theta \| \widehat{p}_t) + 3C_\sigma C_T^{\text{nG}} D_{\text{KL}}(p_t^\theta \| \widehat{p}_t) \\ &\quad + 3C_\sigma \int_{\Omega} \left| f^\theta(x, t) - \mathcal{V}[p_t^\theta](x, t) \right|^2 p_t^\theta(x) dx \\ &\leq \left(6C_\sigma \|\nabla \log \widehat{p}_t\|_\infty^2 \|U\|_\infty^2 + 4\|U\|_\infty \left\| \frac{\nabla^2 \widehat{p}_t}{\widehat{p}_t} \right\|_\infty + 3C_\sigma C_T^{\text{nG}} \right) D_{\text{KL}}(p_t^\theta \| \widehat{p}_t) \\ &\quad + 3C_\sigma \int_{\Omega} \left| f^\theta(x, t) - \mathcal{V}[p_t^\theta](x, t) \right|^2 p_t^\theta(x) dx. \end{aligned}$$

By Gronwall inequality, we obtain that

$$\sup_{t \in [t_0, T]} D_{\text{KL}}(p_t^\theta \| \widehat{p}_t) \leq \left(3C_\sigma \int_{t_0}^t \int_{\Omega} \left| f^\theta(x, t) - \mathcal{V}[p_t^\theta](x, t) \right|^2 p_t^\theta(x) dx dt \right) \exp \{ \bar{C} T \},$$

where

$$(3.16) \quad \bar{C} = \begin{cases} 3 \left(2C_\sigma (C_K)^2 + C_\sigma C_T^{\text{nG}} \right), & \text{Interaction 1,} \\ \max_{t \in [t_0, T]} \left(6C_\sigma \|\nabla \log \widehat{p}_t\|_\infty^2 \|U\|_\infty^2 + 4\|U\|_\infty \left\| \frac{\nabla^2 \widehat{p}_t}{\widehat{p}_t} \right\|_\infty \right) + 3C_\sigma C_T^{\text{nG}}, & \text{Interaction 2,} \end{cases}$$

□

3.5. Proof of Theorem 3.4.

Proof of Theorem 3.4. For convenience and simplicity, we write $X_{t_0, t}^*$, $X_{t_0, t}^N$ as X_t^* , X_t^N . For $t_0 \leq t \leq t_0 + (N_T - 1)\Delta t$, using Taylor expansion and the smoothness of the velocity $\mathcal{V}[\widehat{p}_t]$, we have

$$\begin{aligned} (3.17) \quad X_{t+\Delta t}^*(x) &= X_t^*(x) + \mathcal{V}[\widehat{p}_t](X_t^*(x), t) \Delta t + \frac{d^2 X_t^*(x)}{2 dt^2} \Big|_{t=\tau} (\Delta t)^2 \\ &= X_t^*(x) + \frac{d^2 X_t^*(x)}{2 dt^2} \Big|_{t=\tau} (\Delta t)^2 + \left(b(X_t^*, t) + \int_{\Omega} K(X_t^*(x) - y) \widehat{p}_t(y) dy \right. \\ &\quad - \int_{\Omega} F(r, t) \nu(dr) - \frac{1}{2} \Sigma(X_t^*(x), t) - \frac{1}{2} \Sigma(X_t^*(x), t) \nabla \log \widehat{p}_t(X_t^*(x)) \\ &\quad \left. + \int_{|r| < 1} F(r, t) \frac{\int_0^1 \widehat{p}_t(X_t^*(x) - \lambda F(r, t)) d\lambda}{\widehat{p}_t(X_t^*(x))} \nu(dr) \right) \Delta t, \end{aligned}$$

for some $\tau \in [t, t + \Delta t]$. According to Algorithm 3.1, we have

$$(3.18) \quad X_{t+\Delta t}^N(x) = X_t^N(x) + \Delta t \left[b(X_t^N(x), t) - s(X_t^N(x), t) - \int_{|r|<1} F(r, t) \nu(dr) - \nabla \cdot \frac{\Sigma(X_t^N(x), t)}{2} \right],$$

where $\{x^{(i)}\}_{i=1}^N$ is a set of N samples from initial density p_{t_0} . Note that $s(x, t)$ is the total ‘‘score’’ term, we could separate it into three parts that correspond to the interaction, diffusion and Lévy losses respectively. Let

$$(3.19) \quad s(x, t) = -s_K(x, t) + \frac{1}{2}\Sigma(x, t)s_B(x, t) - s_L(x, t).$$

Subtracting equation (3.17) by (3.18) we have

$$(3.20) \quad \begin{aligned} X_{t+\Delta t}^*(x) - X_{t+\Delta t}^N(x) &= X_t^*(x) - X_t^N(x) + \frac{d^2 X_t^*(x)}{2 dt^2} \Big|_{t=\tau} (\Delta t)^2 + \nabla b(X_{t,\xi}, t) \\ &\cdot (X_t^*(x) - X_t^N(x)) \Delta t - \frac{1}{2} \nabla \Sigma(X_{t,\xi'}) \cdot (X_t^*(x) - X_t^N(x)) \Delta t + e_K \Delta t - \frac{1}{2} e_B \Delta t + e_L \Delta t, \end{aligned}$$

where e_K , e_B and e_L are given in the following. First, based on the law of large numbers and the assumption that the kernel function is twice-differentiable, for the bounded interaction (1),

$$\begin{aligned} \mathbb{E}_x |e_K| &:= \mathbb{E}_x \left| \int_{\Omega} K(X_t^*(x) - y) \widehat{p}_t(y) dy - s_K(X_t^N(x), t) \right| \\ &\leq \mathbb{E}_x \left| \int_{\Omega} K(X_t^*(x) - y) \widehat{p}_t(y) dy - \int_{\Omega} K(X_t^N(x) - y) \widehat{p}_t(y) dy \right| \\ &\quad + \mathbb{E}_x \left| \int_{\Omega} K(X_t^N(x) - y) \widehat{p}_t(y) dy - s_K(X_t^N(x), t) \right| \leq C_1 \mathbb{E}_x |X_t^*(x) - X_t^N(x)| + \varepsilon, \end{aligned}$$

where $C_1 = 2 \sup_{x \in \Omega} |\nabla \cdot K(x)| < \infty$. For the Biot–Savart interaction (2),

$$\begin{aligned} \mathbb{E}_x |e_K| &\leq \mathbb{E}_x \left| \int_{\Omega} K(X_t^*(x) - y) \widehat{p}_t(y) dy - \int_{\Omega} K(X_t^N(x) - y) \widehat{p}_t(y) dy \right| \\ &\quad + \mathbb{E}_x \left| \int_{\Omega} K(X_t^N(x) - y) \widehat{p}_t(y) dy - s_K(X_t^N(x), t) \right| \\ &= \mathbb{E}_x \left| \int_{\Omega} K(z) \widehat{p}_t(z + X_t^*(x)) dz - \int_{\Omega} K(z) \widehat{p}_t(z + X_t^N(x)) dz \right| \\ &\quad + \mathbb{E}_x \left| \int_{\Omega} K(X_t^N(x) - y) \widehat{p}_t(y) dy - s_K(X_t^N(x), t) \right| \\ &= \mathbb{E}_x \left| \int_{\Omega} -U(z) \cdot \nabla \widehat{p}_t(z + X_t^*(x)) dz + \int_{\Omega} U(z) \cdot \nabla \widehat{p}_t(z + X_t^N(x)) dz \right| \\ &\quad + \mathbb{E}_x \left| \int_{\Omega} K(X_t^N(x) - y) \widehat{p}_t(y) dy - s_K(X_t^N(x), t) \right| \\ &\leq C_2 \mathbb{E}_x |X_t^*(x) - X_t^N(x)| + \varepsilon, \end{aligned}$$

where $C_2 := \sup_{t \in [t_0, T]} \|\nabla_x \left(\int_{\Omega} U(z) \cdot \nabla \widehat{p}_t(z + x) dz \right)\|_{\infty} < \infty$.

Second,

$$\begin{aligned}
|e_B| &:= \left| \Sigma(X_t^*(x), t) \nabla \log \widehat{p}_t(X_t^*(x)) - \Sigma(X_t^N(x), t) s_B(X_t^N(x), t) \right| \\
&\leq \left| \Sigma(X_t^*(x), t) \nabla \log \widehat{p}_t(X_t^*(x)) - \Sigma(X_t^*(x), t) \nabla \log \widehat{p}_t(X_t^N(x)) \right| \\
&\quad + \left| \Sigma(X_t^*(x), t) \nabla \log \widehat{p}_t(X_t^N(x)) - \Sigma(X_t^N(x), t) \nabla \log \widehat{p}_t(X_t^N(x)) \right| \\
&\quad + \left| \Sigma(X_t^N(x), t) \nabla \log \widehat{p}_t(X_t^N(x)) - \Sigma(X_t^N(x), t) s_B(X_t^N(x), t) \right| \\
&\leq C_3 |X_t^* - X_t^N| + \varepsilon,
\end{aligned}$$

where $C_3 = \sup_{t \in [t_0, T]} \sup_{x \in \Omega} (C_\sigma |\nabla^2 \log \widehat{p}_t(x)| + \|\nabla \log \widehat{p}_t\|_\infty |\nabla \cdot \Sigma(x, t)|) < \infty$.

Third,

$$\begin{aligned}
|e_L| &:= \left| \int_{|r| < 1} F(r, t) \frac{\int_0^1 \widehat{p}_t(X_t^*(x) - \lambda F(r, t)) d\lambda}{\widehat{p}_t(X_t^*(x))} \nu(dr) \right. \\
&\quad \left. + \int_{|r| \geq 1} G(r, t) \frac{\int_0^1 \widehat{p}_t(X_t^*(x) - \lambda G(r, t)) d\lambda}{\widehat{p}_t(X_t^*(x))} \nu(dr) - s_L(X_t^N(x), t) \right| \\
&\leq \left| \mathcal{I}_t(\widehat{p}_t, F)(X_t^*(x)) - \mathcal{I}_t(\widehat{p}_t, F)(X_t^N(x)) \right| + \left| \mathcal{I}_t(\widehat{p}_t, G)(X_t^*(x)) - \mathcal{I}_t(\widehat{p}_t, G)(X_t^N(x)) \right| \\
&\quad + \left| \mathcal{I}_t(\widehat{p}_t, F)(X_t^*(x)) - \mathcal{I}_t(\widehat{p}_t, F, G)(X_t^N(x)) - s_L(X_t^N(x), t) \right| \\
&\leq C_4 |X_t^*(x) - X_t^N(x)| + \varepsilon,
\end{aligned}$$

where $C_4 = \sup_{t \in [t_0, T]} C_T^f C_T^* \|\nabla \widehat{p}_t\|_\infty \left(\int_{|r| < 1} |F(t)r| dr + \int_{|r| \geq 1} |G(t)r| dr \right) < \infty$.

Now from (3.20), we have, for some positive constant C ,

$$\begin{aligned}
\mathbb{E}_x |X_{t+\Delta t}^* - X_{t+\Delta t}^N| &\leq \mathbb{E}_x |X_t^* - X_t^N| + C \mathbb{E}_x |X_t^* - X_t^N| \Delta t + \left(\frac{C_1}{\sqrt{N}} + 3\varepsilon \right) \Delta t + \mathcal{O}((\Delta t)^2), \\
C &= \begin{cases} \|\nabla b\|_\infty + \frac{1}{2} \|\Sigma(\cdot, t)\|_\infty + C_1 + C_3 + C_4, & \text{Interaction 1,} \\ \|\nabla b\|_\infty + \frac{1}{2} \|\Sigma(\cdot, t)\|_\infty + C_2 + C_3 + C_4, & \text{Interaction 2.} \end{cases}
\end{aligned}$$

Therefore $\mathbb{E}_x |X_t^* - X_t^N| \leq e^{C(t-t_0)} \mathbb{E}_x |X_{t_0}^* - X_{t_0}^N| + \left[\mathcal{O}\left(\frac{1}{\sqrt{N}}\right) + \mathcal{O}(\varepsilon) + \mathcal{O}(\Delta t) \right] (t - t_0)$, as $\frac{1}{N}$, ε and Δt all tend to 0. With the same initial condition, we immediately obtain (3.14). \square

4. Numerical Experiments. We examine several examples to demonstrate the effectiveness of our algorithm 3.1. The time interval $[0, T]$ is uniformly partitioned into N_T sub-intervals $[t_k, t_{k+1}]$, where $t_k = k \frac{T}{N_T}$ for $k = 0, 1, \dots, N_T$. On each sub-interval $[t_k, t_{k+1}]$, the transport map is approximated by a neural network $s^{\theta_k}(\cdot, t_k) : \mathbb{R}^d \rightarrow \mathbb{R}^d$, modeled as a multi-layer perceptron (MLP) with 3 hidden layers, 32 neurons per layer, and the *Swish* activation function. The algorithm is implemented with the following parameter settings: the time step size of $\Delta t = T/N_T = t_{k+1} - t_k = 10^{-3}$, the time horizon of $T = 1$, and the sample size of $N = 4000$.

The initial condition \widehat{p}_0 of (2.1) in all examples is set as the Gaussian distribution for its simplicity in generating initial samples $\{X_0^{(i)}\}_{i=0}^N$ (unless otherwise specified, it is assumed to be the standard normal distribution). For each time step in training the score function $s^{\theta_{k+1}}(\cdot, t_{k+1})$, we use the warm start for the optimization by initializing the neural network parameter θ_{k+1} by the obtained parameters θ_k^* from the previous

step, followed by the standard the Adam optimizer with a learning rate of 10^{-4} to optimize θ_{k+1} .

To evaluate our method, we use the total variation (TV) distance of the generated samples to compare our method with the Monte Carlo simulation method. At each time t_k , we identify the smallest rectangular domain Ω_{t_k} covering all sample points and discretize it into uniform grid cells $\{\Delta_i\}$. The distribution for each method is then approximated by a histogram: $P(\Delta_i) = \frac{\#(\text{samples} \in \Delta_i)}{\#\text{samples}}$. We denote these binned empirical distributions as P^{MC} for Monte Carlo and P^{S} for our method, and the TV distance between these two distributions is then numerically computed by

$$d_{\text{TV}}(P^{\text{MC}}, P^{\text{S}}) = \sum_i \left| P^{\text{MC}}(\Delta_i) - P^{\text{S}}(\Delta_i) \right|.$$

EXAMPLE 1 (1D Jump-diffusion with finite jump activity). *To test the efficiency of our proposed method, we consider the following one-dimensional SDE:*

$$(4.1) \quad dX_t = \kappa(\eta - X_{t-})dt + \sigma dB_t + J_t dN_t,$$

which has been applied in [9] to model CO₂ emissions and fuel-switching strategies. In this example, we set $\kappa = 1$, $\eta = 1$, and $\sigma = 2$. The process N_t is assumed to be a Poisson process with intensity $\Lambda = 30$, while the jump sizes J_t are drawn from a Gaussian distribution N_{m,v^2} with mean $m = 0.1$ and standard deviation $v = 1/24$. To compare with (2.1), the jump term $J_t dN_t$ is equivalently written as $\int_{\mathbb{R}} r \mathcal{N}(dt, dr)$, i.e., $F(r, t) = G(r, t) = r$, where \mathcal{N} is a Poisson random measure with Lévy measure $\nu(dr) = \Lambda N_{m,v^2}(dr)$, and the numerical integration with respect to $N_{m,v^2}(dr)$ is based on a quadrature formula within a truncated interval $[m - 3v, m + 3v]$.

Figure 1 illustrates the temporal evolution of probability flows and probability density functions for Equation (4.1), obtained via both the Monte Carlo simulation and the proposed method. Specifically, the Monte Carlo simulation employs the following Euler–Maruyama discretization scheme: $X_{t+\Delta t}^{(i)} = X_t^{(i)} + \kappa(\eta - X_t^{(i)})\Delta t + \sigma\xi_t + \sum_{k=1}^{N_{\Delta t}} J_k$, $i = 1, \dots, N$, where $\xi_t \sim N_{0,\Delta t}$, $N_{\Delta t} \sim \text{Po}(\Lambda\Delta t)$ is a Poisson random variable with rate $\Lambda\Delta t$, and J_k 's are i.i.d. random variables for jump sizes distributed as N_{m,v^2} .

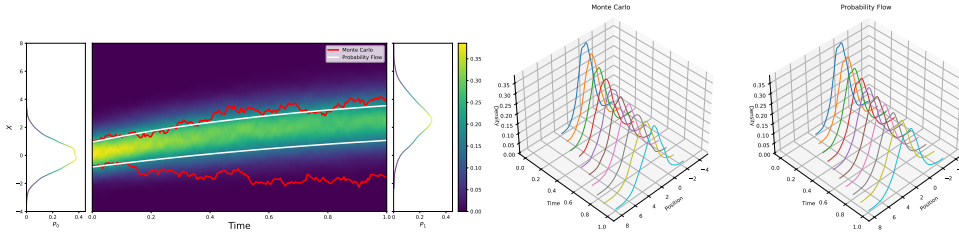


FIG. 1. [Example 1] Probability flows of (4.1). The left panel illustrates the temporal evolution of the probability distribution as a heat map, overlaid with two selective stochastic trajectories based on the Monte Carlo simulation (red) and the two deterministic trajectories based on the transport map (white). The middle and right panels compare the probability distributions $\hat{p}_t(x)$ from the Monte Carlo simulation and the proposed method in the time-state space.

Figure 2 illustrates the TV distance between P^{MC} and P^{S} . The TV distance remains consistently on the order of 10^{-2} , which demonstrates the relative accuracy of our method across time.

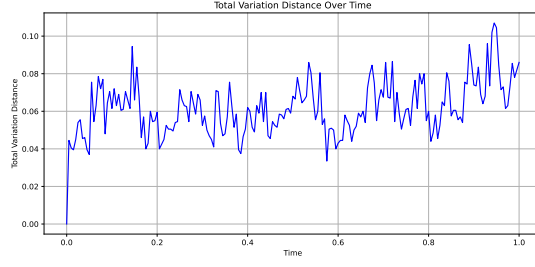


FIG. 2. [Example 1] The TV distance between P^{MC} and P^{S} for (4.1).

EXAMPLE 2 (Jump-diffusion with α -stable Lévy noise). *In this example, we consider the following one-dimensional SDE:*

$$(4.2) \quad dX_t = \kappa(\eta - X_{t-})dt + \sigma dB_t + dL_t^\alpha,$$

which has been widely used to capture dynamics with both continuous fluctuations and heavy-tailed, discontinuous shocks, making them relevant in fields such as finance, physics [2], and generative modeling [41]. This system captures mean reversion, diffusion, and an α -stable Lévy motion L_t^α with Lévy measure:

$$\nu(r) = c_\alpha \frac{1}{|r|^{\alpha+1}}, \quad c_\alpha = \frac{\alpha}{2^{1-\alpha} \sqrt{\pi}} \frac{\Gamma(\frac{1+\alpha}{2})}{\Gamma(1-\frac{\alpha}{2})}, \quad \Gamma(z) := \int_0^\infty t^{z-1} e^{-t} dt.$$

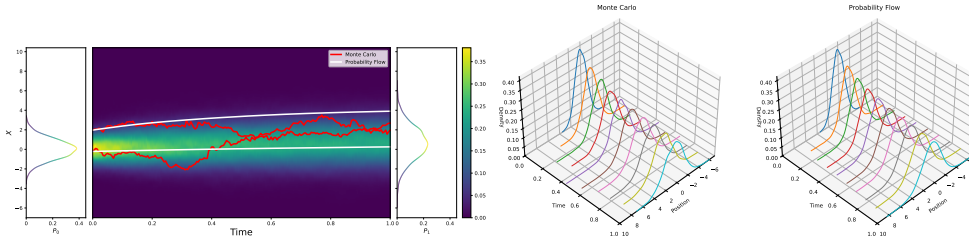


FIG. 3. [Example 2] Probability flows of (4.2).

We set $\alpha = 1.5$ while keeping all other hyperparameters the same as in Example 1. To avoid the singularity of the intensity measure ν at 0, the numerical integration with respect to $\nu(r)$ is restricted to the interval $[-5, -0.01] \cup [0.01, 5]$. In this example, the Monte Carlo simulation is based on the following Euler-Maruyama scheme: $X_{t+\Delta t}^{(i)} = X_t^{(i)} + \kappa(\eta - X_t^{(i)})\Delta t + \sigma\xi_t + \Delta L_t^\alpha$, $i = 1, \dots, N$, where the jump increments $\Delta L_t^\alpha = L_{t+\Delta t}^\alpha - L_t^\alpha$ follow a stable distribution $S_\alpha(\Delta t^{\frac{1}{\alpha}}, 0, 0)$.

Figure 3 and Figure 4 depict the evolutions of probability flow and the TV distance between P^{MC} and P^{S} . The proposed method demonstrates convincing performance in handling α -stable Lévy processes and singular intensity measures, maintaining a TV distance on the order of 10^{-2} .

EXAMPLE 3 (Double-well system with interaction force). *Next, we consider the following two-dimensional interactive SDE:*

$$(4.3) \quad \begin{aligned} dX_t &= (X_{t-} - X_{t-}^3)dt + K * \hat{p}_t(X_{t-})dt + \sigma dB_t^1 + J_t dN_t, \\ dY_t &= Y_{t-}dt + K * \hat{p}_t(Y_{t-})dt + \sigma dB_t^2, \end{aligned}$$

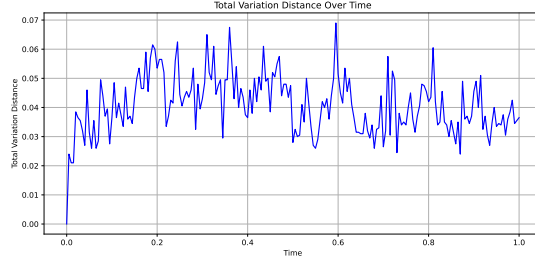


FIG. 4. [Example 2] The TV distance between P^{MC} and P^{S} for (4.2).

where the interaction kernel is $K(x) = x$. We set the parameters σ and J_t to be the same as those in Example 1, and the Monte Carlo simulation is based on the following Euler–Maruyama method:

$$(4.4) \quad \begin{aligned} X_{t+\Delta t}^{(i)} &= X_t^{(i)} + (X_t^{(i)} - (X_t^{(i)})^3)\Delta t + \frac{1}{N} \sum_{j=1}^N K(X_t^{(i)} - X_t^{(j)})\Delta t + \sigma \xi_t^1 + \sum_{k=1}^{N\Delta t} J_k, \\ Y_{t+\Delta t}^{(i)} &= Y_t^{(i)} + Y_t^{(i)}\Delta t + \frac{1}{N} \sum_{j=1}^N K(Y_t^{(i)} - Y_t^{(j)})\Delta t + \sigma \xi_t^2, \quad i = 1, \dots, N, \end{aligned}$$

where ξ_t^1 and ξ_t^2 are independent random variables sampled from the Gaussian distribution $N_{0,\Delta t}$.

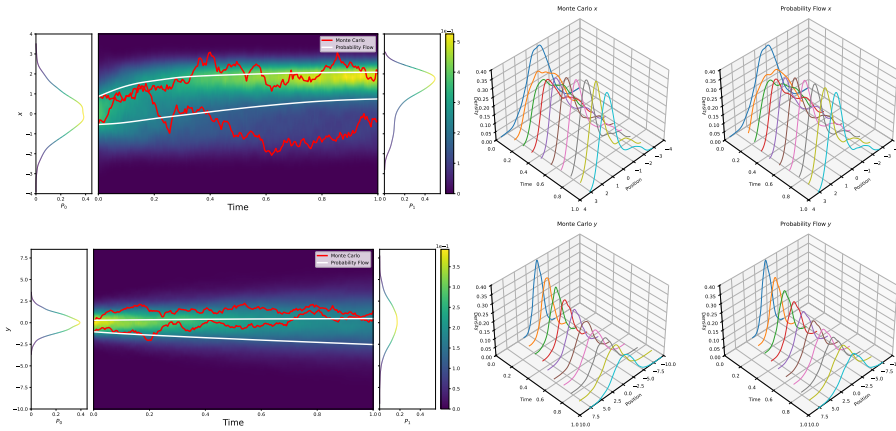


FIG. 5. [Example 3] The Probability flows of (4.3) along the axes: x (top), and y (bottom).

Figure 5 illustrates the evolution of probability flows obtained from Equation (4.3), computed using both the Monte Carlo simulation and the proposed approach. Figure 6 depicts the probability flow evolution on the xy -plane at different time steps for both methods. Finally, Figure 7 presents the TV distance between P^{MC} and P^{S} , consistently demonstrating values on the order of 10^{-2} . These results confirm the accuracy of the proposed method in approximating the probability flows for systems with interaction terms.

EXAMPLE 4 (State-dependent jump-diffusion). To conclude our numerical study, we consider the following three-dimensional SDE which describes the asset price dy-

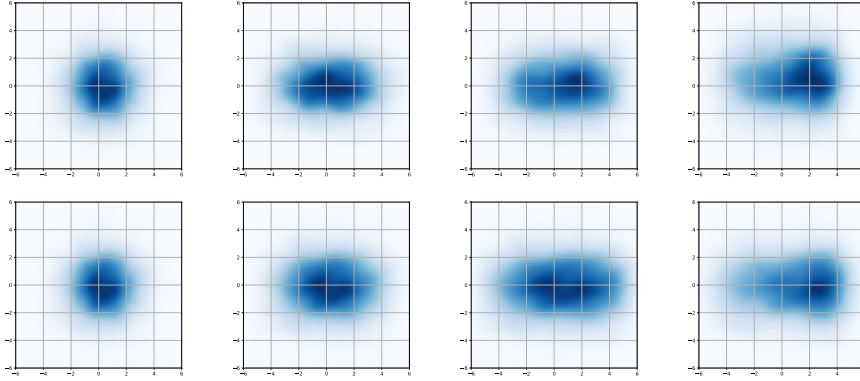


FIG. 6. [Example 3] Kernel density estimation (KDE) of distributions for 4000 samples in the xy -plane. Top: Monte Carlo simulation (4.4); Bottom: results from Algorithm 3.1. From left to right: the distributions are shown at the 0th, 40th, 100th, and 250th time steps.

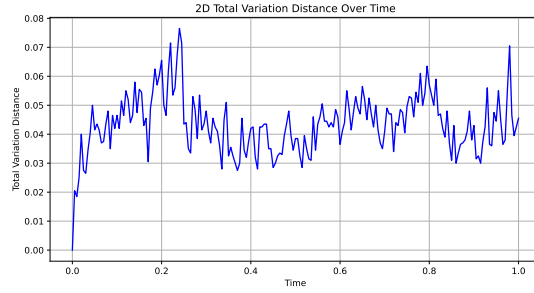


FIG. 7. [Example 3] The TV distance between P^{MC} and P^{S} for (4.3).

namics under both jump and stochastic volatility conditions[23]

$$(4.5) \quad \begin{aligned} ds_t &= (\gamma - \delta - v_{t-}/2 - \Lambda(v_{t-}, m_{t-})\bar{J}) dt + \sqrt{|v_{t-}|} dB_t^1 + \log(J_t^s + 1) dN_t, \\ dv_t &= \kappa_v(m_{t-} - v_{t-}) dt + \sigma_v \sqrt{|v_{t-}|} (dB_t^1 + \sqrt{1 - \rho^2} dB_t^2) + J_t^v dN_t, \\ dm_t &= \kappa_m(\alpha_m - m_{t-}) dt + \sigma_m \sqrt{|m_{t-}|} dB_t^3. \end{aligned}$$

Here $B_t = (B_t^1, B_t^2, B_t^3)$ is the standard Brownian motion in \mathbb{R}^3 and N_t is an independent Poisson process with the state-dependent rate $\Lambda(v, m) = \Lambda_0 + \Lambda_1 v + \Lambda_2 m$. The jump component J_t^v follows the exponential distribution with the expectation μ_j^v . Meanwhile, the jump component for the stock price, J_t^s , follows a shifted log-normal distribution, where $J_t^s + 1$ is characterized by the parameters μ_s and σ_s , leading to $\mathbb{E}(J_t^s) = \bar{J} = \exp(\mu_s + \sigma_s^2/2) - 1$. The parameters are from [23] and specified as follows: $(\gamma, \delta, \kappa_v, \kappa_m, \alpha_m, \sigma_v, \sigma_m, \rho) = (0.04, 0.015, 3.1206, 3.3168, 0.1125, 0.394, 0.0835, -0.688)$, $(\Lambda_0, \Lambda_1, \Lambda_2) = (2.096, 21.225, 0)$, and $(\mu_s, \sigma_s, \mu_j^v) = (-0.012, 0.043, 0.002)$.

We set the initial condition as a three-dimensional Gaussian distribution with the mean vector $(5, 5, 5)^\top$ and the covariance matrix of a 3×3 identity matrix. The numerical integration for r is performed over a two-dimensional uniform grid defined on $[-0.17, 0.17] \times [0, 0.0015]$, which is designed to capture the critical density features

required for accurate numerical evaluation. The Monte Carlo approximation is easy to achieve by noting that the numerical approximation of $\log(J_t^s + 1) dN_t$ is $\sum_{k=1}^{N_{\Delta t}} \xi_k^{J^s}$ where $\{\xi_k^{J^s}\}_{k \in \mathbb{N}}$ are i.i.d samples from the law of $\log(J_t^s + 1)$ and $N_{\Delta t} \sim Po(\Lambda \Delta t)$. Similarly $J_t^v dN_t$ is approximated by $\sum_{k=1}^{N_{\Delta t}} \xi_k^{J^v}$ where $\{\xi_k^{J^v}\}_{k \in \mathbb{N}}$ are i.i.d samples from the law of J_t^v .

Let $X_t = (s_t, v_t, m_t)^\top$, the SDE (4.5) can be rewritten as

$$dX_t = \left[\begin{pmatrix} \gamma - \delta - \lambda_0 \bar{J} \\ 0 \\ \kappa_m \alpha_m \end{pmatrix} + \begin{pmatrix} 0 & -1/2 - \Lambda_1 \bar{J} & -\Lambda_2 \bar{J} \\ 0 & -\kappa_v & \kappa_v \\ 0 & 0 & -\kappa_m \end{pmatrix} X_t \right] dt + \begin{pmatrix} \sqrt{|v_t|} & 0 & 0 \\ \sigma_v \sqrt{|v_t|} & \sigma_v \sqrt{|v_t|} \sqrt{1 - \rho^2} & 0 \\ 0 & 0 & \sigma_m \sqrt{|m_t|} \end{pmatrix} dB_t + \int_{\mathbb{R}^3} \begin{pmatrix} \log(r_1 + 1) \\ r_2 \\ 0 \end{pmatrix} \mathcal{N}(dt, dr),$$

where \mathcal{N} denotes a random Poisson measure on $\mathbb{R}_+ \times \mathbb{R}^3$ with Lévy measure $dt \times \Lambda(v_t, m_t) \nu_J(dr)$, and the jump-size measure $\nu_J(dr) = \nu_{J^s}(dr_1) \times \nu_{J^v}(dr_2) \times \nu_{J^m}(dr_3)$. In this expression, $F(r, t) = G(r, t) = (\log(r_1 + 1), r_2, 0)^\top$.

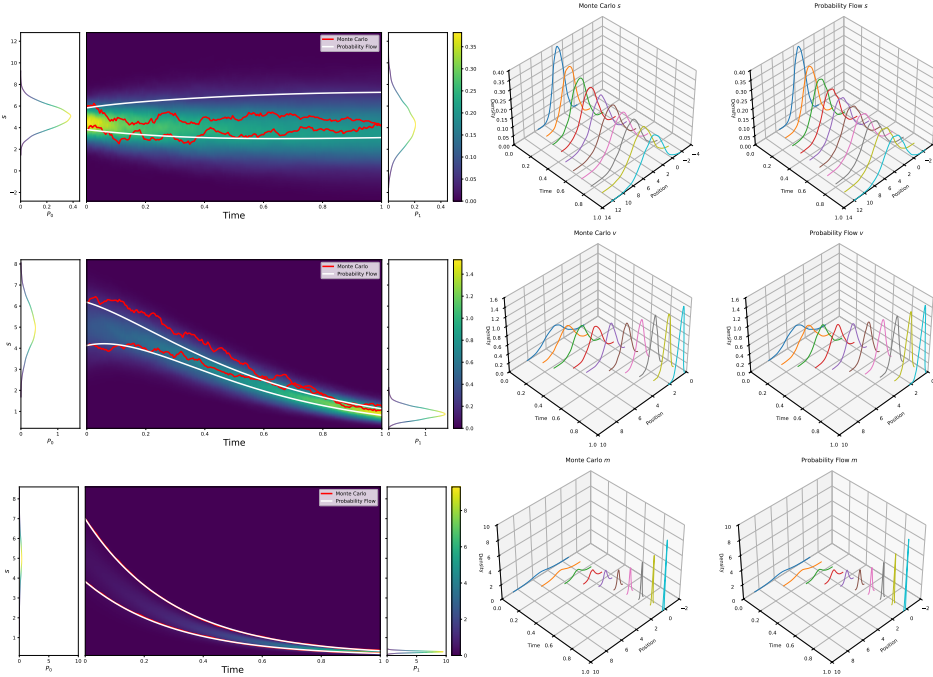


FIG. 8. [Example 4] Probability flows along the axes: s (top), v (middle), and m (bottom).

Figure 8 illustrates the evolution of probability flows for each marginal derived from Equation (4.5). Figure 9 presents the TV distance between the probabilities P^{MC} and P^{S} , demonstrating that the distance remains on the order of 10^{-2} . These results highlight the capability of our proposed method to accurately and efficiently solve complex state-dependent jump-diffusion systems.

5. Conclusions. In this paper, we introduced the concept of the *generalized score function*, which unifies the conventional diffusion score and the Lévy score, thereby accommodating a broad class of non-Gaussian processes. Leveraging this generalized score function, we developed a score-based particle algorithm to efficiently

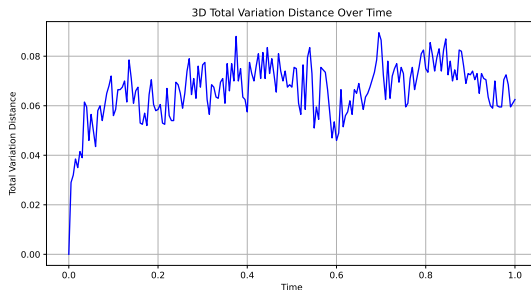


FIG. 9. [Example 4] The TV distance between P^{MC} and P^{S} for (4.5).

solve the nonlinear Lévy-Fokker-Planck equation through sampling of probability flow data. Furthermore, we demonstrate that the Kullback-Leibler divergence between the numerical solution and the ground truth is bounded by a specific loss function, derived from a fixed-point perspective. The rigorous numerical analysis was conducted to validate the theoretical properties of our algorithm. Finally, several numerical examples were presented to illustrate the effectiveness and accuracy of the proposed method.

Data Availability. The datasets generated and/or analyzed during the current study are available in the GitHub repository, accessible via the following link: <https://github.com/cliu687/sbtm-levy>. All scripts and supporting files necessary to reproduce the findings are openly provided in this repository.

REFERENCES

- [1] D. APPLEBAUM, *Lévy processes and stochastic calculus*, Cambridge university press, 2009.
- [2] T. ARIGA, K. TATEISHI, M. TOMISHIGE, AND D. MIZUNO, *Noise-induced acceleration of single molecule kinesin-1*, Physical review letters, 127 (2021), p. 178101.
- [3] P. BARTHELEMY, J. BERTOLOTTI, AND D. S. WIERSMA, *A Lévy flight for light*, Nature, 453 (2008), pp. 495–498.
- [4] N. M. BOFFI AND E. VANDEN-ELJNDEN, *Probability flow solution of the Fokker–Planck equation*, Machine Learning: Science and Technology, 4 (2023), p. 035012.
- [5] N. M. BOFFI AND E. VANDEN-ELJNDEN, *Deep learning probability flows and entropy production rates in active matter*, P NATL ACAD SCI USA, 121 (2024), p. e2318106121.
- [6] L. CAFFARELLI AND L. SILVESTRE, *An extension problem related to the fractional Laplacian*, Communications in partial differential equations, 32 (2007), pp. 1245–1260.
- [7] Y. CAO, J. CHEN, Y. LUO, AND X. ZHOU, *Exploring the optimal choice for generative processes in diffusion models: Ordinary vs stochastic differential equations*, Advances in Neural Information Processing Systems, 36 (2024).
- [8] H. CHEN, H. LEE, AND J. LU, *Improved analysis of score-based generative modeling: User-friendly bounds under minimal smoothness assumptions*, in Proceedings of the 40th International Conference on Machine Learning, vol. 202, 2023, pp. 4735–4763.
- [9] J. CHEVALLIER AND S. GOUTTE, *Estimation of Lévy-driven Ornstein–Uhlenbeck processes: Application to modeling of CO2 and fuel-switching*, Annals of Operations Research, 255 (2017), pp. 169–197.
- [10] V. DE BORTOLI, J. THORNTON, J. HENG, AND A. DOUCET, *Diffusion Schrödinger bridge with applications to score-based generative modeling*, in Advances in Neural Information Processing Systems, vol. 34, Curran Associates, Inc., 2021, pp. 17695–17709.
- [11] P.-E. C. DE RAYNAL, J.-F. JABIR, AND S. MENOZZI, *Multidimensional stable driven McKean–Vlasov SDEs with distributional interaction kernel: a regularization by noise perspective*, Stochastics and Partial Differential Equations: Analysis and Computations, (2024), pp. 1–54.
- [12] D. GALLON, A. JENTZEN, AND P. VON WURSTEMBERGER, *An overview of diffusion models for*

- generative artificial intelligence*, arXiv preprint arXiv:2412.01371, (2024).
- [13] F. GOLSE, *On the dynamics of large particle systems in the mean field limit*, Macroscopic and large scale phenomena: coarse graining, mean field limits and ergodicity, (2016), pp. 1–144.
 - [14] G. GOTTWALD, F. LI, Y. MARZOUK, AND S. REICH, *Stable generative modeling using diffusion maps*, arXiv preprint arXiv:2401.04372, (2024).
 - [15] J. HO, A. JAIN, AND P. ABBEEL, *Denosing diffusion probabilistic models*, in Advances in Neural Information Processing Systems, vol. 33, Curran Associates, Inc., 2020, pp. 6840–6851.
 - [16] Z. HU, Z. ZHANG, G. E. KARNIADAKIS, AND K. KAWAGUCHI, *Score-fPINN: Fractional score-based physics-informed neural networks for high-dimensional Fokker-Planck-Lévy equations*, arXiv preprint arXiv:2406.11676, (2024).
 - [17] Y. HUANG AND L. WANG, *A score-based particle method for homogeneous Landau equation*, arXiv preprint arXiv:2405.05187, (2024).
 - [18] Y. HUANG, X. ZHOU, AND J. DUAN, *Probability flow approach to the Onsager–Machlup functional for jump-diffusion processes*, SIAM Applied Math(accepted). arXiv:2409.01340.
 - [19] A. HYVÄRINEN AND P. DAYAN, *Estimation of non-normalized statistical models by score matching.*, Journal of Machine Learning Research, 6 (2005).
 - [20] V. ILIN, J. HU, AND Z. WANG, *Transport based particle methods for the Fokker-Planck-Landau equation*, ArXiv, abs/2405.10392 (2024).
 - [21] P.-E. JABIN AND Z. WANG, *Quantitative estimates of propagation of chaos for stochastic systems with $W^{-1,\infty}$ kernels*, Inventiones mathematicae, 214 (2018), pp. 523–591.
 - [22] K. KANAZAWA, T. G. SANO, A. CAIROLI, AND A. BAULE, *Loopy Lévy flights enhance tracer diffusion in active suspensions*, Nature, 579 (2020), pp. 364–367.
 - [23] D. KRISTENSEN, Y. J. LEE, AND A. MELE, *Closed-form approximations of moments and densities of continuous-time Markov models*, Journal of Economic Dynamics and Control, (2024), p. 104948.
 - [24] L. LI, S. HURAUULT, AND J. SOLOMON, *Self-consistent velocity matching of probability flows*, in Thirty-seventh Conference on Neural Information Processing Systems, 2023.
 - [25] M. LIANG, M. B. MAJKA, AND J. WANG, *Exponential ergodicity for SDEs and Mckean–Vlasov processes with Lévy noise*, Annales de l’Institut Henri Poincaré (B) Probabilités et statistiques, 57 (2021), pp. 1665–1701.
 - [26] H. LIU AND J. Y. LIN, *Stochastic Mckean–Vlasov equations with Lévy noise: Existence, attractiveness and stability*, Chaos, Solitons & Fractals, 177 (2023), p. 114214.
 - [27] Y. LIU, M. YANG, Z. ZHANG, F. BAO, Y. CAO, AND G. ZHANG, *Diffusion-model-assisted supervised learning of generative models for density estimation*, Journal of Machine Learning for Modeling and Computing, 5 (2024).
 - [28] J. LU, Y. WU, AND Y. XIANG, *Score-based transport modeling for mean-field Fokker-Planck equations*, Journal of Computational Physics, 503 (2024), p. 112859.
 - [29] D. MAOUTSA, S. REICH, AND M. OPPER, *Interacting particle solutions of Fokker–Planck equations through gradient–log–density estimation*, Entropy, 22 (2020), p. 802.
 - [30] C. OLIVERA AND M. SIMON, *Microscopic derivation of non-local models with anomalous diffusions from stochastic particle systems*, arXiv preprint arXiv:2404.03772, (2024).
 - [31] F. SANTAMBROGIO, *Optimal transport for applied mathematicians*, Birkäuser, NY, 55 (2015).
 - [32] Z. SHEN AND Z. WANG, *Entropy-dissipation informed neural network for Mckean–Vlasov type PDEs*, Advances in Neural Information Processing Systems, 36 (2024).
 - [33] Z. SHEN, Z. WANG, S. KALE, A. RIBEIRO, A. KARBASI, AND H. HASSANI, *Self-consistency of the Fokker–Planck equation*, in Conference on Learning Theory, PMLR, 2022, pp. 817–841.
 - [34] J. SONG, C. MENG, AND S. ERMON, *Denosing diffusion implicit models*, in International Conference on Learning Representations, 2021.
 - [35] M. S. SONG, H. C. MOON, J.-H. JEON, AND H. Y. PARK, *Neuronal messenger ribonucleoprotein transport follows an aging Lévy walk*, Nature communications, 9 (2018), pp. 1–8.
 - [36] Y. SONG AND S. ERMON, *Generative modeling by estimating gradients of the data distribution*, in NeurIPS, vol. 32, Curran Associates, Inc., 2019.
 - [37] Y. SONG, S. GARG, J. SHI, AND S. ERMON, *Sliced score matching: A scalable approach to density and score estimation*, in Uncertainty in Artificial Intelligence, PMLR, 2020, pp. 574–584.
 - [38] Y. SONG, J. SOHL-DICKSTEIN, D. P. KINGMA, A. KUMAR, S. ERMON, AND B. POOLE, *Score-based generative modeling through stochastic differential equations*, International Conference on Learning Representations (ICLR), (2021).
 - [39] T. TOMÉ AND M. OLIVEIRA, *Stochastic Dynamics and Irreversibility*, Graduate Texts in Physics, Springer International Publishing, 2014.
 - [40] C. VILLANI ET AL., *Optimal transport: old and new*, vol. 338, Springer, 2009.
 - [41] E. B. YOON, K. PARK, S. KIM, AND S. LIM, *Score-based generative models with Lévy processes*, Advances in Neural Information Processing Systems, 36 (2023), pp. 40694–40707.